

# Accepted Manuscript

$\beta$ -Carboline and *N*-hydroxycinnamamide hybrids as anticancer agents for drug-resistant hepatocellular carcinoma

Yong Ling, Wei-Jie Gao, Changchun Ling, Ji Liu, Chi Meng, Jianqiang Qian, Siqun Liu, Huiling Gan, Hongmei Wu, Jinhua Tao, Hong Dai, Yanan Zhang



PII: S0223-5234(19)30168-0

DOI: <https://doi.org/10.1016/j.ejmech.2019.02.054>

Reference: EJMECH 11146

To appear in: *European Journal of Medicinal Chemistry*

Received Date: 29 November 2018

Revised Date: 15 January 2019

Accepted Date: 17 February 2019

Please cite this article as: Y. Ling, W.-J. Gao, C. Ling, J. Liu, C. Meng, J. Qian, S. Liu, H. Gan, H. Wu, J. Tao, H. Dai, Y. Zhang,  $\beta$ -Carboline and *N*-hydroxycinnamamide hybrids as anticancer agents for drug-resistant hepatocellular carcinoma, *European Journal of Medicinal Chemistry* (2019), doi: <https://doi.org/10.1016/j.ejmech.2019.02.054>.

This is a PDF file of an unedited manuscript that has been accepted for publication. As a service to our customers we are providing this early version of the manuscript. The manuscript will undergo copyediting, typesetting, and review of the resulting proof before it is published in its final form. Please note that during the production process errors may be discovered which could affect the content, and all legal disclaimers that apply to the journal pertain.

## $\beta$ -Carboline and *N*-hydroxycinnamamide hybrids as anticancer agents for drug-resistant hepatocellular carcinoma

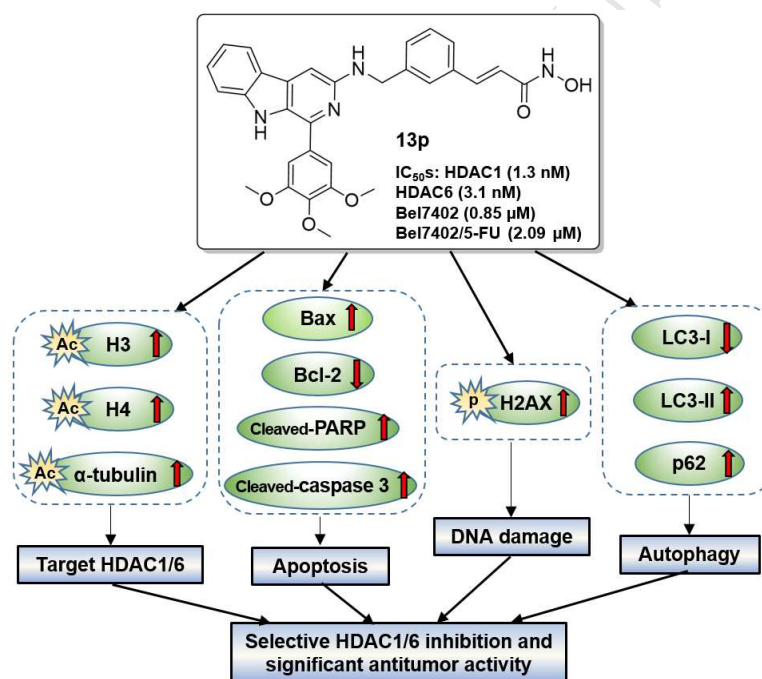
Yong Ling <sup>a,b</sup>, Wei-Jie Gao <sup>a</sup>, Changchun Ling <sup>a,b</sup>, Ji Liu <sup>a</sup>, Chi Meng <sup>a</sup>, Jianqiang Qian <sup>a</sup>, Siqun Liu <sup>a</sup>, Huiling Gan <sup>a</sup>, Hongmei Wu <sup>a</sup>, Jinhua Tao <sup>a</sup>, Hong Dai <sup>a,c,\*</sup>, Yanan Zhang <sup>a,\*</sup>

<sup>a</sup>School of Pharmacy and Jiangsu Province Key Laboratory for Inflammation and Molecular Drug Target, Nantong University, Nantong 226001, PR China.

<sup>b</sup>The Affiliated Hospital of Nantong University, Nantong University, Nantong 226001, PR China.

<sup>c</sup>College of Chemistry and Chemical Engineering, Nantong University, Nantong 226019, PR China

### Graph Abstract



# **$\beta$ -Carboline and *N*-hydroxycinnamamide hybrids as anticancer agents for drug-resistant hepatocellular carcinoma**

Yong Ling<sup>a,b</sup>, Wei-Jie Gao<sup>a</sup>, Changchun Ling<sup>a,b</sup>, Ji Liu<sup>a</sup>, Chi Meng<sup>a</sup>, Jianqiang Qian<sup>a</sup>, Siqun Liu<sup>a</sup>, Huiling Gan<sup>a</sup>, Hongmei Wu<sup>a</sup>, Jinhua Tao<sup>a</sup>, Hong Dai<sup>a,c,\*</sup>, Yanan Zhang<sup>a,\*</sup>

<sup>a</sup>School of Pharmacy and Jiangsu Province Key Laboratory for Inflammation and Molecular Drug Target, Nantong University, Nantong 226001, PR China.

<sup>b</sup>The Affiliated Hospital of Nantong University, Nantong University, Nantong 226001, PR China.

<sup>c</sup>College of Chemistry and Chemical Engineering, Nantong University, Nantong 226019, PR China

**Abstract:** In an effort to develop anticancer agents that may overcome drug resistance, the number one reason in cancer death, we have developed a series of novel hybrids of  $\beta$ -carboline and *N*-hydroxycinnamamide as histone deacetylase (HDAC) inhibitors. Most of the hybrids **13a-p** showed strong antiproliferative effects with low-micromolar IC<sub>50</sub> values against four human cancer cells. The most potent compound of the series **13p** exhibited high HDAC1/6 inhibitory effects, and also increased the acetylation levels of histone H3, H4 and  $\alpha$ -tubulin. Importantly, **13p** demonstrated high anticancer potency against drug-sensitive HepG2 and Bel7402 cells and drug-resistant Bel7402/5FU cells. Hybrid **13p** triggered significant apoptosis by regulating apoptotic relative proteins expression in these Bel7402/5FU cells. Finally, **13p** induced a substantial amount of autophagic flux activity by the accretion of the expression of LC3-II and the degeneration of expression of p62 and LC3-I in Bel7402/5FU cells. Overall, **13p** is a novel  $\beta$ -carboline/*N*-hydroxycinnamamide hybrid with significant anticancer potency that warrants further evaluation for the treatment of drug-resistant hepatocellular carcinoma.

**Keywords:** Histone deacetylase inhibitors; Hybrids; *N*-Hydroxycinnamamide;  $\beta$ -Carbolines; Drug resistance.

## **1. Introduction**

Cancer represents a major health threat in both developed and under developed countries. According to the report of World Health Organization, an estimated 9 million patients died of malignant tumor in the whole world in 2015 [1]. Tumor resistance has severely limited the effectiveness of many current chemotherapeutic agents. Despite the great advances in chemotherapy, particularly molecularly targeted therapeutics, many types of cancers that are initially susceptible to chemotherapy can develop resistance over time through various mechanisms. Currently 90% of failures in chemotherapy occur during the invasion and metastasis of cancers related to drug resistance and most patients have to succumb to the recurrent drug-resistant disease [2]. There is a pressing need to develop novel therapeutic agents to overcome the limitations of currently available therapies, particularly the development of drug

---

\* Corresponding author. Tel.: +86-513-85051892; e-mail: zhangyanan@gmail.com, dh123@ntu.edu.cn

resistance [3-6].

The majority of anticancer agents can trace their original or underlying synthetic design principles to natural products [7], including many widely used antitumor drugs such as paclitaxel, teniposide, camptothecin and vincristine [8].  $\beta$ -Carbolines are a family of alkaloids found in plants and animals, and are an important class of natural products widely distributed in nature. Many  $\beta$ -carbolines, including harmine and its analogs harmaline and harmalol, have been traditionally used for the prevention and treatment of multiple cancers or malaria [9-11]. While  $\beta$ -carbolines generally show weak anti-cancer effects [12], structurally modified derivatives have been shown to have improved antitumor activities [13]. Studies by our group and others showed that hybrid molecules bearing a  $\beta$ -carboline and another antitumor entity such as a histone deacetylase (HDAC) inhibitor may result in synergistic effects and increased anticancer efficacy [14,15]. Interestingly, harmine was also found to reduce resistance to anticancer drugs such as camptothecin and mitoxantrone, which were mediated by breast cancer resistance protein (BCRP) [16].

Hybrid drug molecules, designed to simultaneously modulate multiple oncogenic signaling pathways with a single molecule, offer a promising alternate strategy that may overcome some of the many disadvantages of single cancer drugs such as multi-drug resistance. HDACs have been a promising candidate for hybrid agent development [17], since they are clinically validated cancer targets and HDAC inhibitors demonstrated prominent antitumor efficacy on broad spectrum neoplasms in preclinical and clinical studies [18,19]. For example, HDAC inhibitor belinostat (PXD101) and cisplatin, when used together, have been found to exert synergistic cytotoxic effect against cisplatin-resistant lung cancer cell lines, suggesting HDAC inhibitors as novel agents for drug resistance reversal in combination chemotherapeutic regimens [20]. Therefore, introduction of HDAC inhibitor structural moieties to  $\beta$ -carbolines may not only increase the potency, but also reverse drug resistance, the number one reason in cancer death.

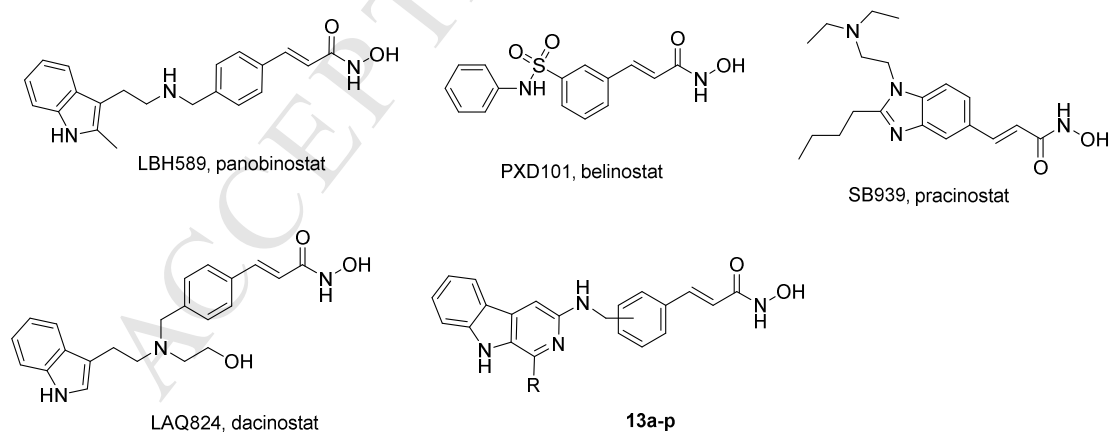


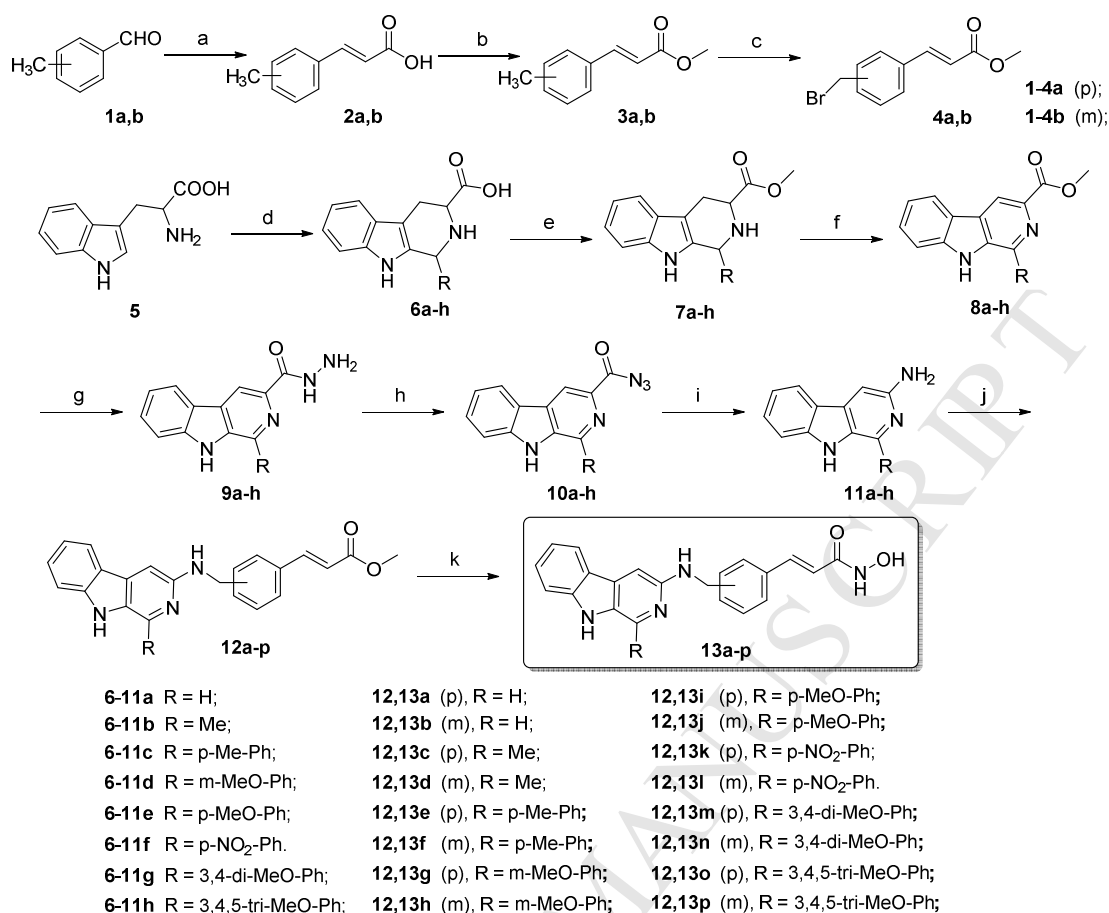
**Fig. 1.** Structures of representative *N*-hydroxycinnamide based HDAC inhibitors and  $\beta$ -carboline/*N*-hydroxycinnamide hybrids **13a-p**.

A number of HDAC inhibitors have been either approved by the FDA or currently in clinical stages, many of which have an *N*-hydroxycinnamide as an important active fragment (Figure 1). These include belinostat, panobinostat (LBH589) and pracinostat (SB939), all of which are FDA

approved drugs for the treatment of peripheral T-cell lymphoma or multiple myeloma [21], and dacinostat (LAQ824), which entered clinical trials [22] (Fig. 1). HDACi's have been known to induce autophagy and apoptosis, two forms of programmed cell death that are responsible for the turnover/degradation of organelles and proteins within cells and of cells within organisms [23]. HDACi's commonly induce apoptosis through either the extrinsic (death receptor on cell surface) pathway, involving ligands such as Fas or TNF-related apoptosis-inducing ligand (TRAIL) and proteins such as FAS-associated death domain (FADD) and caspase-8, or the intrinsic (mitochondria) pathway, involving proteins such as the Bcl-2 superfamily. Similarly, several signaling pathways have been suggested to play important roles in regulating HDAC-induced autophagy, including mTOR, AIF, ROS, CDKs, and HDAC1/6 [24–26]. In addition,  $\beta$ -carboline have also been reported to show antitumor activities via inducing both apoptosis and autophagy [27–29]. Therefore, incorporation of the HDAC inhibiting *N*-hydroxycinnamamide moiety into the  $\beta$ -carboline may lead to hybrid molecules with increased anticancer potency/efficacy. Since these HDAC inhibitors all bear an aromatic ring-containing group on the *N*-hydroxycinnamamide group, we reasoned that replacement of this aromatic group with an aromatic  $\beta$ -carboline may retain the HDAC activity. In addition, the introduction of the  $\beta$ -carboline group with anti-tumor activities may also render synergistic effects to these hybrids. Since the aromatic ring-containing group is at either the meta or para position of the *N*-hydroxycinnamamide in these HDAC inhibitors, we will investigate both of these substitution patterns with the  $\beta$ -carbolines. We herein report our progress on the synthesis and discovery of  $\beta$ -carboline/*N*-Hydroxycinnamamide hybrids **13a-p**.

## 2. Results and discussion

### 2.1 Chemistry



**Scheme 1.** Preparation of compounds **13a-p**: (a) malonic acid, DMF, piperidine, reflux, 4 h, 80-87%; (b) sulfoxide chloride, methanol, 0 °C, 1 h, and 65 °C 4 h, 87-91%; (c) NBS, AIBN, CCl<sub>4</sub>, rt, 2 h, 65-72%; (d) H<sup>+</sup> or OH<sup>-</sup>, R-CHO, reflux, 2-4 h, 71-86%; (e) sulfoxide chloride, methanol, 0 °C, 1 h, and 65 °C 4-6 h, 82-90%; (f) potassium permanganate, N,N-dimethylformamide, rt, 2-6 h, 61-76%; (g) hydrazine monohydrate, methanol, 0 °C, 1 h, 84-95%; (h) NaNO<sub>2</sub>, HCl, H<sub>2</sub>O, 0 °C, 6 h; (i) HAc, H<sub>2</sub>O, reflux, 6h, 56-71%; (j) **4a,b**, K<sub>2</sub>CO<sub>3</sub>, CH<sub>3</sub>CN, 50 °C, 3-5h, 65-78%; (k) NH<sub>2</sub>OK, methanol, rt, 8-12h, 47-58%.

The preparation route of target compounds **13a-p** is presented in Scheme 1. The key intermediates **4a,b** were synthesized in three steps. The starting 3- and 4-methyl benzaldehydes **1a,b** were converted to cinnamic acids **2a,b** in a Knoevenagel condensation reaction with the treatment of malonic acid. Cinnamic acids **2a,b** were converted to the corresponding esters **3a,b** under standard esterification conditions using MeOH and SOCl<sub>2</sub>. Bromination of **3a,b** via a free radical reaction using N-bromosuccinimide (NBS) and catalyzed by azodiisobutyronitrile (AIBN) afforded the benzyl bromides **4a,b**. Next, L-tryptophan **5** underwent a Pictet-Spengler condensation reaction with different aldehydes to generate **6a-h**, which were then converted to methyl esters **7a-h**. Treatment of esters **7a-h** with potassium permanganate in N,N-dimethylformamide produced intermediates **8a-h**, which were then converted to β-carboline hydrazides **9a-h** when treated with hydrazine monohydrate. Treatment of **9a-h** with NaNO<sub>2</sub> accomplished the conversion of the hydrazide group to an acyl azide group to afford intermediates **10a-h**. The acyl azide in compounds **10a-h** was converted to an amino group in the presence of HAc in H<sub>2</sub>O via Curtius rearrangement to afford compounds **11a-h**. Reaction between **11a-h** and methyl

bromomethyl-cinnamate **4a,b** in the presence of  $K_2CO_3$  in  $CH_3CN$  produced key intermediates **12a-p**. Finally, the target compounds **13a-p** were prepared by the reaction of intermediates **12a-p** with  $NH_2OK$  in MeOH. The structure of all final compounds were confirmed using MS,  $^1H$  NMR,  $^{13}C$  NMR and HRMS. All target compounds had purity of > 95% as determined using HPLC.

### 3. Results and discussion

#### 3.1. HDAC1 inhibitory activity

It was our hypothesis that replacement of the aromatic ring on *N*-hydroxycinnamamide of HDAC inhibitors such as belinostat, panobinostat and pracinostat with a  $\beta$ -carboline subunit would retain their activity. To confirm this was indeed the case, all target compounds **13a-p** were first screened for their HDAC1 inhibitory effect. HDAC1 is a key HDAC subtype and has been indicated in cancer cell proliferation, differentiation, and tissue malignant proliferation. As seen in Table 1, the  $\beta$ -carboline, harmine, showed little HDAC1 inhibitory activity ( $IC_{50} > 1000$  nM), consistent with previous reports. However, all of compounds **13a-p** exhibited significant HDAC inhibitory effects with nanomolar  $IC_{50}$  values.

The structure-activity relationship of compounds **13a-p** clearly revealed that the HDAC1 inhibitory activities of the series are clearly dependent on the substituents at the C1 position. Compounds **13c,d** with a methyl group or **13a,b** with a hydrogen displayed weak HDAC1 inhibition. However, the potencies were enhanced when aryl groups were introduced at the C1 position. In particular, compounds with a phenyl group bearing electron-donating substituents such as a methoxyl group (**13g-j**) or two or more methoxyl groups (**13m-p**) displayed greater HDAC1 inhibitory potencies than the rest compounds. Compound **13p** was the most potent compound of the series and its  $IC_{50}$  value (1.3 nM against HDAC1) was >100-fold lower than the FDA approved HDAC inhibitor SAHA.

#### 3.2. Antiproliferative activities of target compounds

Given the apparent HDAC inhibitory activities of these compounds, some of which are even more potent than SAHA, these target compounds would possess potent antitumor activities, as expected with HDAC inhibitors. To examine their inhibitory activity on cancer cell growth, all target compounds **13a-p** were first screened in the MTT assay against human colon cancer cells (HCT116), human hepatocellular carcinoma cells (HepG2 and SMMC-7721), and human lung cancer cells (H1299). Their  $IC_{50}$  values are summarized in Table 1. Harmine and SAHA were also tested for comparison.

**Table 1.**  $IC_{50}$  values of hybrids **13a-p** against four human cancer cell lines and HDAC1<sup>a</sup>

Compd	R	m or p	HDAC1 $IC_{50}$ (nM)	<i>In vitro</i> antiproliferative activity ( $IC_{50}^a$ , $\mu$ M)			
				SUMM-7721	Hep G2	HCT116	H1299
SAHA	/	/	142 $\pm$ 18	5.23 $\pm$ 0.48	5.94 $\pm$ 0.73	4.97 $\pm$ 0.56	7.02 $\pm$ 0.65
Harmine	/	/	>1000	47.6 $\pm$ 5.12	53.6 $\pm$ 5.50	43.8 $\pm$ 3.85	ND <sup>b</sup>
<b>13a</b>	H	p	197 $\pm$ 18	>12.5	>12.5	>12.5	>12.5
<b>13b</b>	H	m	161 $\pm$ 15	>12.5	>12.5	>12.5	>12.5
<b>13c</b>	Me	p	122 $\pm$ 14	10.6 $\pm$ 0.92	>12.5	11.3 $\pm$ 1.07	>12.5
<b>13d</b>	Me	m	93 $\pm$ 9	7.35 $\pm$ 0.80	8.81 $\pm$ 1.02	9.12 $\pm$ 0.76	8.93 $\pm$ 0.61
<b>13e</b>	4-Me-Ph	p	65 $\pm$ 9	2.99 $\pm$ 0.41	3.46 $\pm$ 0.48	3.31 $\pm$ 0.29	2.95 $\pm$ 0.36

<b>13f</b>	4-Me-Ph	m	81 ± 10	5.19 ± 0.70	6.17 ± 0.52	4.99 ± 0.58	6.32 ± 0.71
<b>13g</b>	3-MeO-Ph	p	1.8 ± 0.3	1.01 ± 0.14	0.72 ± 0.10	1.36 ± 0.18	1.25 ± 0.21
<b>13h</b>	3-MeO-Ph	m	5.2 ± 0.9	2.42 ± 0.31	1.23 ± 0.17	1.96 ± 0.30	1.39 ± 0.24
<b>13i</b>	4-MeO-Ph	p	26 ± 4	3.23 ± 0.39	2.80 ± 0.33	4.29 ± 0.46	2.78 ± 0.32
<b>13j</b>	4-MeO-Ph	m	9.7 ± 1	2.51 ± 0.30	1.96 ± 0.24	2.47 ± 0.28	3.03 ± 0.42
<b>13k</b>	4-NO <sub>2</sub> -Ph	p	20 ± 3	2.18 ± 0.21	1.62 ± 0.15	2.95 ± 0.32	2.46 ± 0.30
<b>13l</b>	4-NO <sub>2</sub> -Ph	m	13 ± 2	1.75 ± 0.15	1.27 ± 0.16	1.68 ± 0.20	2.22 ± 0.26
<b>13m</b>	3,4-(MeO) <sub>2</sub> -Ph	p	24 ± 4	5.46 ± 0.49	3.85 ± 0.43	4.91 ± 0.61	7.06 ± 0.58
<b>13n</b>	3,4-(MeO) <sub>2</sub> -Ph	m	9.3 ± 2	4.10 ± 0.56	3.41 ± 0.47	4.33 ± 0.52	6.11 ± 0.53
<b>13o</b>	3,4,5-(MeO) <sub>3</sub> -Ph	p	5.6 ± 0.7	1.59 ± 0.14	1.55 ± 0.18	1.23 ± 0.14	1.90 ± 0.22
<b>13p</b>	3,4,5-(MeO) <sub>3</sub> -Ph	m	1.3 ± 0.2	1.01 ± 0.10	0.41 ± 0.06	0.87 ± 0.11	0.69 ± 0.10

<sup>a</sup> Related data appeared as the means ± SD of three separated assays. <sup>b</sup> ND: not detected.

As shown in Table 1, most hybrids showed good antiproliferative potencies in all 4 cells, with IC<sub>50</sub>'s in the low micromolar range. Among them, compounds **13e**, **13g-l**, and **13o,p** (IC<sub>50</sub> = 0.41-4.29 μM) demonstrated better antiproliferative potencies than SAHA (IC<sub>50</sub> = 4.97-7.02 μM). Consistent with literature reports, harmine displayed weak anti-cancer potency. These results indicate that the designed structural hybridization resulted in molecules with good to excellent antiproliferative properties. Furthermore, the relative spatial arrangement of the substituted β-carboline moiety and *N*-hydroxycinnamamide had little impact on the potency, with the meta analogs generally exerting a slightly stronger growth inhibitory activity than those with the para position substitutions (e.g. **13m** vs. **13n**, and **13o** vs. **13p**).

In comparing the enzymatic activities with cell viabilities, it is apparent that the relative HDAC1 potencies of these hybrids matched well with their cell based antiproliferation. These results suggest that the antiproliferative properties of this series of hybrids result largely from their HDAC inhibitory activities. Given the strong inhibitory activity of **13p** against tumor cells *in vitro*, we further examined its inhibitory effects on the growth of normal liver cells LO2. It was found that **13p** had weak inhibitory effect on non-tumor LO2 cells with an IC<sub>50</sub> value of 2.83 μM, which was nearly seven-fold weaker than the HepG2 cells (IC<sub>50</sub> = 0.41 μM).

### 3.3. **13p** displays antiproliferative effects against 5-FU drug sensitive and resistance cells

Drug resistance is a leading cause for the failure of many anticancer chemotherapeutic agents [30,31]. To investigate whether these hybrids with potent antiproliferative activities against 4 cancer cells also affect drug resistance, the most potent compounds **13g,h**, **13k,l**, and **13o,p** were further assayed for their activity against drug-sensitive hepatocellular carcinoma (HCC) Bel7402 and the 5-fluorouracil-resistant HCC Bel7402/5-FU cells in the MTT assay. These Bel7402/5-FU cells have been shown to display multi-drug resistance with cross-resistance to many drugs including adriamycin, vincristine, and oxaliplatin [32]. As shown in Table 2, all these compounds displayed significant antiproliferative effects in both cells, with IC<sub>50</sub> values in the low micromolar levels and lower than both SAHA and 5-FU. Notably, **13p** demonstrated the greatest anti-proliferative effects with IC<sub>50</sub> values of 0.85 and 2.09 μM against the drug-sensitive Bel7402 and drug-resistant Bel7402/5-FU cell lines. These values were nearly five- to six-fold better than SAHA (IC<sub>50</sub> = 4.72-9.83 μM) and eighteen- to thirty-fold more potent than 5-FU (IC<sub>50</sub> = 15.6-61.7 μM). In comparison, compound **12p**, an intermediate of **13p**, exhibited weaker antiproliferative

activity than **13p** in both cells, confirming the importance of the hydroxamic acid.

5-FU is one of the most widely used antitumor drugs against colon, liver, and lung cancers. While the mechanisms of 5-FU resistance have not been fully understood, a number of mechanisms have been proposed such as overexpression of target enzyme thymidylate synthetase (TS), high metabolism of 5-FU through the overexpression of dihydropyrimidine dehydrogenase (DPD), and increase of the efflux of 5-FU from cancer cells through ATP-binding cassette (ABC) transporters [33–35]. While further studies are clearly needed, the significant potency displayed by these hybrids in drug-sensitive and drug-resistant cells probably resulted from the synergistic effects between the HDAC inhibitor and the  $\beta$ -carboline component. In fact, a number of studies have demonstrated that HDACi's enhance or potentiate 5-FU cytotoxicity, via mechanisms including down-regulation of thymidylate synthase in human cancer cells, or upregulation of major histocompatibility complex class II and p21 genes and activates caspase-3/7 [33-35]. In addition, CUDC-907, a dual HDAC and PI3K inhibitor enhanced the efficacy of 5-FU when used in combination in colorectal cancer cells [36], similar to our results described here.

**Table 2.** IC<sub>50</sub> values of compounds **13g,h**, **13k,l**, and **13o,p** against drug-sensitive HCC Bel7402 and drug-resistant HCC Bel7402/5-FU cells <sup>a</sup>

Compd.	IC <sub>50</sub> <sup>a</sup> , $\mu$ M	
	Bel7402	Bel7402/5-FU
SAHA	4.72 $\pm$ 0.61	9.83 $\pm$ 0.89
5-FU	15.6 $\pm$ 2.03	61.7 $\pm$ 8.45
<b>13g</b>	1.03 $\pm$ 0.12	2.17 $\pm$ 0.26
<b>13h</b>	2.15 $\pm$ 0.23	2.90 $\pm$ 0.35
<b>13k</b>	3.24 $\pm$ 0.35	4.38 $\pm$ 0.56
<b>13l</b>	2.71 $\pm$ 0.40	3.06 $\pm$ 0.29
<b>13o</b>	1.97 $\pm$ 0.26	3.66 $\pm$ 0.48
<b>13p</b>	0.85 $\pm$ 0.13	2.09 $\pm$ 0.30
<b>12p</b>	12.7 $\pm$ 1.53	16.2 $\pm$ 1.95

<sup>a</sup>These data are from three independent experiments, and are presented as the mean  $\pm$  SD.

### 3.4. HDAC subtype selectivity

In addition to HDAC1, several other members of the HDAC family have been indicated in cancer, including HDAC3, HDAC6, and HDAC8. In fact, it has been suggested that the potential side effects of HDAC inhibitors depend largely on the subtype selectivity of the compounds [37]. Therefore, the compounds that showed the best potency for HDAC1 inhibition, including **13g**, **13h**, **13o**, and **13p**, were further evaluated for their inhibitory activities against HDAC3/6/8 (Table 3). This was accomplished by measuring the fluorescent-based enzyme activity of human recombinant HDAC3/6/8 enzymes. These four compounds possessed high inhibitory effects against HDAC6 with IC<sub>50</sub> values of 2.8-7.3 nM, which were significantly lower than SAHA. However, these compounds showed moderate HDAC3 inhibition and weak HDAC8 inhibition. Notably, the most potent compound of the series **13p** exhibited high HDAC1/6 inhibitory effects. This selectivity of **13p** for HDAC1/6 may result from its active fragment *N*-hydroxycinnamide, which not only can form bi-chelation with the active Zn<sup>2+</sup> binding site with its hydroxamic acid group, but also can possibly form sandwich-like  $\pi$ - $\pi$  interactions by inserting its vinyl benzene

group into the two parallel phenylalanine residues of HDAC1/6, as previously reported [38]. In addition, the cap group ( $\beta$ -carboline) may also contribute to the observed HDAC1/6 selectivity. Due to the flexibility of loops in the cap region of HDAC1 and HDAC6, many *N*-containing polyaromatics as cap groups, such as quinazolines and  $\beta$ -carbolines, can comfortably occupy the surface groove and interact with the amino acid residues present at the surface of the HDACs [39].

**Table 3.** IC<sub>50</sub> values of hybrids **13g**, **13h**, **13o**, and **13p** against HDAC1, HDAC3, HDAC6, and HDAC8<sup>a</sup>

Compd.	IC <sub>50</sub> (nM) <sup>a</sup>			
	HDAC1	HDAC3	HDAC6	HDAC8
SAHA	142 ± 18	153 ± 17	65 ± 7	425 ± 51
<b>13g</b>	1.8 ± 0.3	76 ± 9	2.8 ± 0.3	617 ± 55
<b>13h</b>	5.2 ± 0.9	83 ± 9	4.5 ± 0.6	>1000
<b>13o</b>	5.6 ± 0.7	185 ± 21	7.3 ± 0.9	>1000
<b>13p</b>	1.3 ± 0.2	146 ± 18	3.1 ± 0.5	>1000

<sup>a</sup> These data are from three independent experiments, and are expressed as the mean ± SD.

### 3.5. Acetylated histone H3/4 and $\alpha$ -tubulin induced by **13p**.

To confirm that these hybrids induce acetylation of histones at the cellular level, the most potent compound of the series, **13p**, was analyzed in western blotting assays for its effect on the expression level of the Ac-H3, Ac-H4, and Ac- $\alpha$ -tubulin.  $\beta$ -Actin was used as a control (Fig. 2). Drug resistant HCC Bel7402/5-FU cells were incubated for 72h with the vehicle, SAHA (5.0  $\mu$ M), or **13p** (0.8, 2.0, and 5.0  $\mu$ M). The levels of Ac-H3/4, and Ac- $\alpha$ -tubulin relative to  $\beta$ -actin were tested by densitometric scanning.

It is well known that  $\alpha$ -tubulin is the target of HDAC6 and histones H3 and H4 are the targets of HDAC1 and HDAC2. Compounds **13p** significantly enhanced the levels of Ac-H3 and Ac-H4, in agreement with its HDAC1 activity in the enzymatic assay. In addition, **13p** also increased the expression of Ac- $\alpha$ -tubulin, consistent with the observed high 6 activities. These results also suggest that **13p** was cell permeable. Consistent with the above HDAC isoform fluorimetric assay results, most of the **13p** treated groups (2.0 and 5.0  $\mu$ M) showed higher levels of Ac-H3, Ac-H4, and Ac- $\alpha$ -tubulin, than the 5.0  $\mu$ M SAHA treated group.

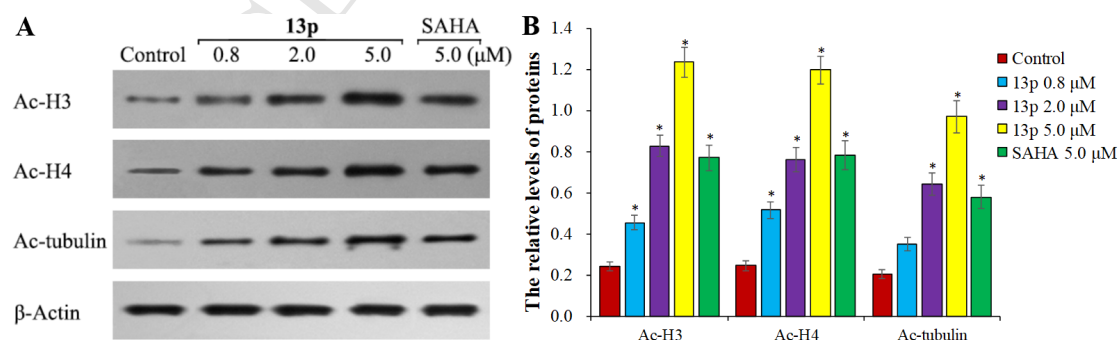


**Fig. 2.** Treatment with **13p** enhanced histone H3/4 and  $\alpha$ -tubulin acetylation in vitro. (A) Western blotting analysis in Bel7402/5-FU cells treated with **13p** and SAHA. (B) Quantitative analysis. These data are from three separate experiments, and are presented as means ± SD. \**P* < 0.01 vs control.

### 3.6. Tumor cell apoptosis induction of **13p**

Since it displayed selective HDAC1/6 inhibitory effects and remarkable HCC cell antiproliferative activities, we next investigated whether **13p** leads to enhanced cancer cell apoptosis, a common mechanism for antiproliferation. Thus, Bel7402/5-FU cells were incubated for 72h with of **13p** (2.0 or 5.0  $\mu\text{M}$ ), SAHA, or harmine, respectively, and then screened with FITC-Annexin V/PI staining and flow cytometry to analyze the percentages of apoptotic cells. In Fig. 3, the percentages of apoptotic Bel7402/5-FU cells (53.42% for 2.0  $\mu\text{M}$  and 71.05% for 5.0  $\mu\text{M}$ ) increased with the increasing concentrations of **13p**, suggested increased apoptosis. These values were higher than both the SAHA (30.78% for 5.0  $\mu\text{M}$ ) and harmine (23.36% for 20  $\mu\text{M}$ ) groups, agreeing with above results.

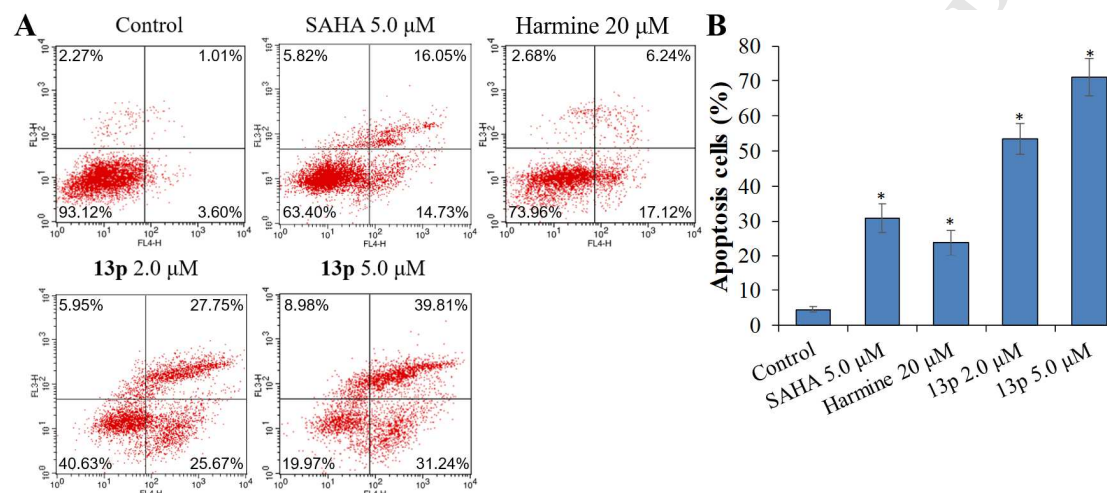


**Fig. 3.** Compound **13p** induces Bel7402/5-FU cell apoptosis *in vitro*. (A) Flow cytometry analysis of Bel7402/5-FU cells treated **13p**, SAHA, or harmine, respectively, and stained with FITC-Annexin V/PI. (B) Quantitative analysis of percentages of apoptotic cells. Related data appeared as the means  $\pm$  SD of three separated assays. \* $P < 0.01$  vs control.

We next determined the expression of several key apoptotic proteins, including Bax and Bcl-2, and the cleavage states of caspase-3 and PARP (apoptosis markers), upon **13p** treatment (Fig. 4). Thus, Western blotting assay was performed using subconfluent Bel7402/5-FU HCC cells treated with or without **13p**, SAHA, or harmine for 72h. The levels of protein expression were then detected using specific antibodies. As depicted in Fig. 4, treatment with **13p** markedly increased the expression of pro-apoptotic Bax while reducing the expression of the antiapoptotic Bcl-2 protein. Importantly, **13p** led to cleavage of PARP and caspase-3 to a greater degree than the control group, and also greater than the SAHA group. Together, these results indicate that **13p** could significantly promote cancer cell apoptosis in drug-resistant Bel7402/5-FU cells.

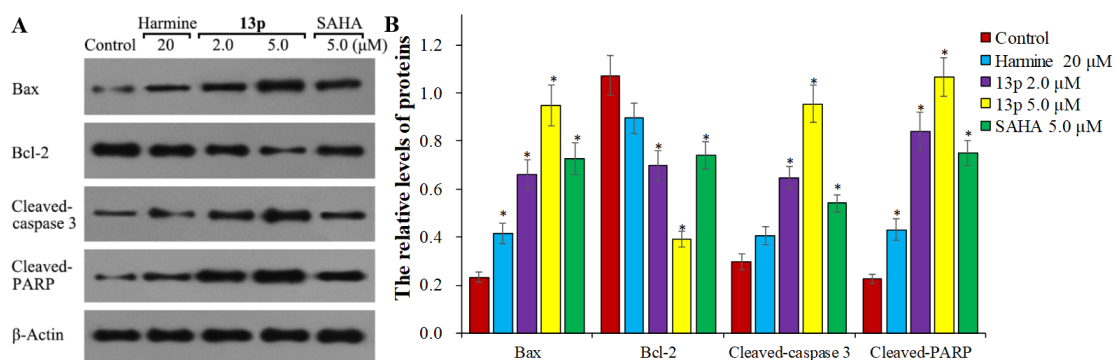


**Fig. 4.** (A) The levels of Bax, Bcl-2, cleaved Caspase 3, PARP and  $\beta$ -actin in Bel7402/5-FU cells treated with **13p**, SAHA, or harmine in Western blotting assay. (B) Quantitative analysis of the relative levels of each protein (Bax, Bcl-2, cleaved-caspase 3, and cleaved-PARP) compared to  $\beta$ -actin. Related data appeared as the means  $\pm$  SD of three separated assays. \* $P < 0.01$  vs control.

### 3.7. Compound **13p** induces DNA damage

$\beta$ -Carbolines have been reported to bind and induce DNA damage, thanks to the planar skeleton [40]. We therefore investigated DNA damage induced by **13p** in Bel7402/5-FU cells, which may contribute to the anti-cancer potency of these  $\beta$ -carboline/N-hydroxycinnamamide hybrids. Histone H2AX phosphorylation was used as the DNA damage marker. Thus, Bel7402/5-FU cells were treated with vehicle or **13p** for 72 h and their lysates were analyzed using specific antibodies. H2AX (S139ph) levels were determined using western blotting analysis. Harmine and SAHA were also tested in parallel. As shown in Fig. 5, **13p** dose-dependently enhanced the levels of phosphorylated H2AX in Bel7402/5-FU cells, which was significantly better than both the harmine and SAHA group. Therefore, these results clearly support that the hybrids are involved in DNA damage.

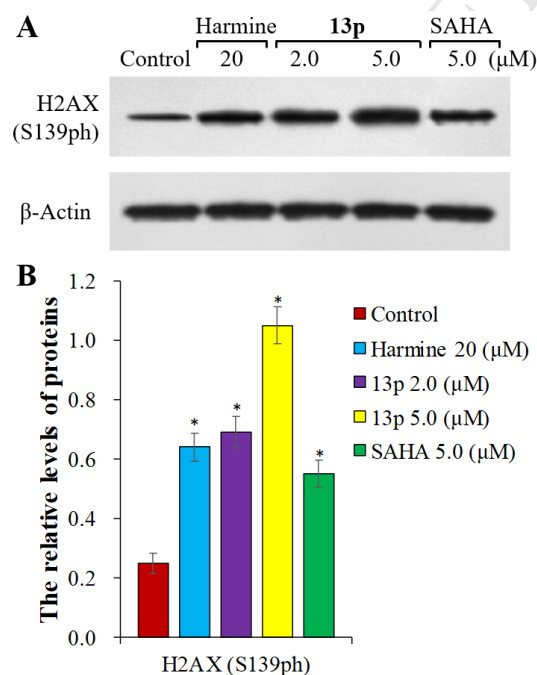


**Fig. 5.** DNA damage in western blotting assay. (A) H2AX levels, relative to  $\beta$ -Actin, in Bel7402/5-FU cells treated with **13p**, SAHA, or harmine. (B) Quantitative analysis. The data of three separate experiments are presented as

means  $\pm$  SD from. \*P < 0.01 vs control.

### 3.8. Compound **13p** induces autophagy in Bel7402/5-FU cells

Autophagy is an intracellular catabolic process that targets damaged and superfluous cellular proteins, organelles, and other cytoplasmic components to maintain metabolism and homeostasis [41]. The role of autophagy in cancer is context dependent, but studies in genetically engineered mouse models suggest that autophagy can constrain tumor initiation by regulating DNA damage and oxidative stress [42-44]. Autophagy can be induced by numerous cytotoxic compounds. To examine whether **13p** affects autophagy in Bel7402/5-FU cells, we used acridine orange (AO) staining to detect autophagic formation using fluorescence microscopy. As shown in Fig. 6, green fluorescence was primarily emitted in control cells with weak red fluorescence, highlighting a low autophagic induction. By contrast, cells treated with **13p** displayed a dose-dependent rise in red fluorescence, while **13p** sharply decreased the green fluorescence intensity. These results indicate a substantial amount of the autophagosome accumulations in **13p**-treated groups in Bel7402/5-FU cells, which was more than the harmine- and SAHA-treated groups.

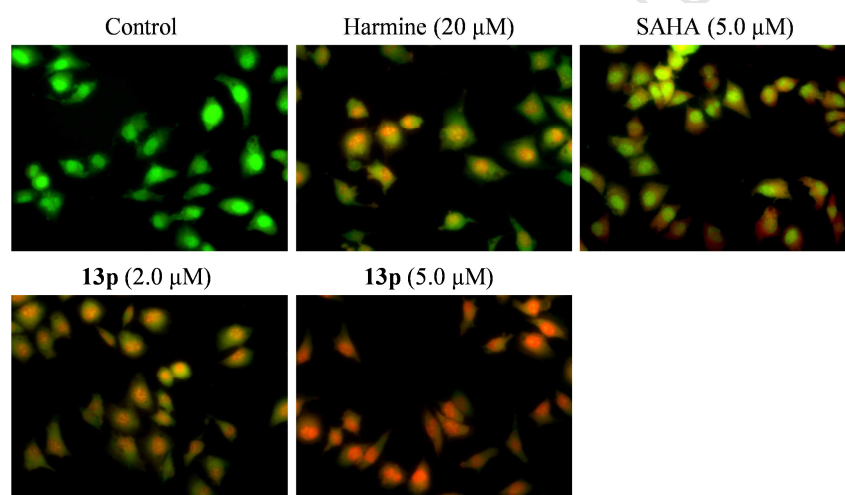


**Fig. 6.** Detection of autophagic vacuoles in Bel7402/5-FU cells after various treatments for 24 h; (a) control cells; (b) harmine for 20  $\mu$ M, (c) SAHA for 5.0  $\mu$ M and (d) **13p**-treated cells (2.0 and 5.0  $\mu$ M). The level of acridine orange staining was determined by fluorescence microscopy. Representative images were captured from three independent experiments under 400  $\times$  magnification.

The induction of autophagy was further studied by assessing the levels of key autophagy-associated proteins. The transformation of LC3-I into LC3-II is a key step in autophagy and the number of autophagosomes correlates to the number of LC3-II puncta. We therefore examined the expression of autophagy-associated proteins LC3-I, LC3-II and p62, in response to **13p** treatment (Fig. 7). Thus, Bel7402/5-FU cells were incubated with, or without **13p**, harmine, and SAHA at the indicated doses for 72h and the levels of protein were analyzed using specific antibodies. Western blotting assay showed that **13p** markedly enhanced the expression of LC3-II in a dose-dependent manner, which were better than that in harmine- and SAHA-treated groups (Fig. 7B), while expression of p62 decreased after treatment with different concentrations of **13p** for 72h.

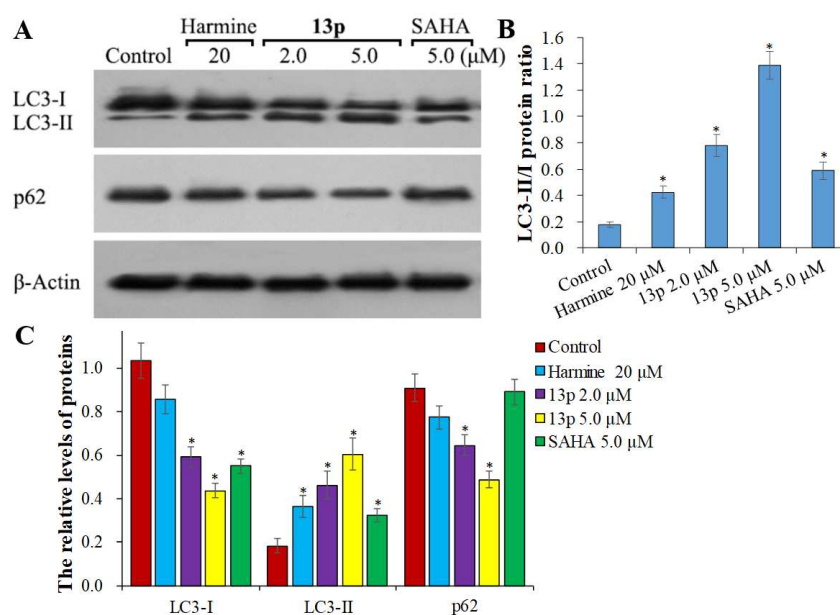


**Fig. 7.** (A) The expression of autophagy-related proteins LC3 and p62 as analyzed in western blotting assay in Bel7402/5-FU cells treated with **13p**, SAHA, or harmine. (B) Quantitative analysis of the relative levels of LC3 and p62 compared to control  $\beta$ -actin. Related data appeared as the means  $\pm$  SD of three separated assays. \* $P < 0.01$  vs respective control.

#### 4. Conclusions

In summary, we have designed and prepared a series of novel hybrids based on  $\beta$ -carboline and N-hydroxycinnamamide **13a-p**, and evaluated their in vitro anticancer activities and anticancer mechanisms in a battery of assays. Most of these compounds had enhanced inhibitory potency against HDAC1 and also exerted selective HDAC6 inhibition. They also displayed low micromolar antiproliferative potencies against 4 different human cancer cells, including **13p** which exhibited strong and selective antiproliferative activities against both drug-sensitive HepG2, Bel7402 and drug-resistant Bel7402/5FU cells. Further, **13p** caused accumulation of acetylated histones and acetylated  $\alpha$ -tubulin, confirming their HDAC inhibitory activities. In addition, **13p** also displayed greater potency in inducing Bel7402/5FU cell apoptosis than SAHA and harmine by enhancing the expression of cleaved caspase-3 and PARP proteins. In addition, **13p** induced a substantial amount of autophagic flux activity in Bel7402/5FU cells by up-regulation of LC3-II proteins and down-regulation of p62 and LC3-I, more significant than both the harmine- and SAHA-treated groups. In summary, these results suggest that the novel  $\beta$ -carboline/N-hydroxycinnamamide hybrids described here may be potential candidates for the development of novel antitumor agents in the treatment of human cancer, especially those with multi-drug resistance.

#### 5. Experimental protocols

##### 5.1. Chemical analysis

All compounds were synthesized and purified by column chromatography containing silica gel (300–400 mesh) or by recrystallization. TLC analysis was performed by silica gel GF<sub>254</sub> plates

(250 mm; Qingdao O. C. C., China).  $^1\text{H}$  NMR and  $^{13}\text{C}$  NMR spectra were collected on a Bruker AV 400M spectrometer in  $\text{CDCl}_3$  or  $\text{DMSO-}d_6$  and TMS was used as the internal standard. Mass Spectra was recorded on a Mariner Mass Spectrum (ESI). High resolution mass spectrometry (HRMS) were recorded with Agilent technologies LC/MSD TOF. Compounds **4** were prepared according to the procedures described in literatures [45]. Compounds **6-11** were prepared following the procedures in literature [14,46].

## 5.2. General preparation of **12a-p**.

To a solution of compound **4** (4.5 mmol) in 50 ml acetonitrile, was added **11** (8.2 mmol),  $\text{K}_2\text{CO}_3$  (6.0 mmol), and KI (0.7 mmol) at 50 °C for 8h. After the reaction completed, the reaction mixture was concentrated, and the residue was gathered through extraction and concentration, and further purified through quick column chromatography to yield compounds **12a-p**.

Compound **12a**: Yield 71%, MS (ESI)  $m/z = 358.2$   $[\text{M}+\text{H}]^+$ . Analytical data for **12a**: Yellow solid;  $^1\text{H}$  NMR ( $d_6$ -DMSO, 400 MHz)  $\delta$  7.91 (t, 1H, Ar-H), 7.66 (d,  $J = 7.4$  Hz, 4H, Ar-H), 7.61 (dd,  $J = 16.0$  Hz, 1H, CH=CH), 7.47 - 7.38 (m, 1H, Ar-H), 7.35 (d,  $J = 8.2$  Hz, 1H, Ar-H), 7.10 - 6.99 (m, 2H, Ar-H), 6.59 (d,  $J = 16.0$  Hz, 1H, CH=CH), 4.88 (s, 2H,  $\text{CH}_2$ ), 3.71 (s, 3H,  $-\text{OCH}_3$ ), 2.66 (m, 3H,  $\text{CH}_3$ ).

Compound **12b**: Yield 68%, MS (ESI)  $m/z = 358.2$   $[\text{M}+\text{H}]^+$ .  $^1\text{H}$  NMR ( $d_6$ -DMSO, 400 MHz)  $\delta$  10.95 (s, 1H, NH), 7.90 (t, 1H, Ar-H), 7.64 (d,  $J = 7.4$  Hz, 4H, Ar-H), 7.61 (dd,  $J = 15.2$  Hz, 1H, CH=CH), 7.47 - 7.38 (m, 1H, Ar-H), 7.35 (d,  $J = 8.2$  Hz, 1H, Ar-H), 7.18 - 6.96 (m, 2H, Ar-H), 6.59 (d,  $J = 15.2$  Hz, 1H, CH=CH), 4.86 (s, 2H,  $\text{CH}_2$ ), 3.69 (s, 3H,  $-\text{OCH}_3$ ), 2.68 (m, 3H,  $\text{CH}_3$ ).

Compound **12c**: Yield 65%, MS (ESI)  $m/z = 372.2$   $[\text{M}+\text{H}]^+$ .  $^1\text{H}$  NMR ( $d_6$ -DMSO, 400 MHz)  $\delta$ : 10.97 (s, 1H, NH), 7.93-7.95 (d, 1H,  $J = 8$  Hz, Ar-H), 7.61-7.67 (m, 4H, NH, Ar-H), 7.34-7.43 (m, 3H, CH=, Ar-H), 7.05-7.06 (m, 2H, Ar-H), 6.57-6.61 (d, 1H,  $J = 16.0$  Hz, CH=), 4.88 (s, 2H,  $\text{CH}_2$ ), 3.71 (s, 3H,  $\text{OCH}_3$ ), 2.63 (s, 3H,  $\text{CH}_3$ ).

Compound **12d**: Yield 68%, MS (ESI)  $m/z = 372.2$   $[\text{M}+\text{H}]^+$ .  $^1\text{H}$  NMR ( $d_6$ -DMSO, 400 MHz)  $\delta$ : 10.97 (s, 1H, NH), 7.94-7.96 (d, 1H,  $J = 8.0$  Hz, Ar-H), 7.35-7.64 (m, 7H, CH=, NH, Ar-H), 7.02-7.06 (m, 2H, Ar-H), 6.52-6.56 (d, 1H,  $J = 16.0$  Hz, CH=), 4.90 (s, 2H,  $\text{CH}_2$ ), 3.70 (s, 3H,  $\text{OCH}_3$ ), 2.65 (s, 3H,  $\text{CH}_3$ ).

Compound **12e**: Yield 60%, MS (ESI)  $m/z = 448.2$   $[\text{M}+\text{H}]^+$ .  $^1\text{H}$  NMR ( $d_6$ -DMSO, 400 MHz)  $\delta$ : 10.77 (s, 1H, NH), 8.03 (d, 1H,  $J = 8.0$  Hz, Ar-H), 7.85-7.87 (m, 2H, Ar-H), 7.60-7.68 (m, 3H, NH, Ar-H), 7.34-7.49 (m, 6H, CH=, Ar-H), 7.09-7.11 (m, 2H, Ar-H), 6.60 (d, 1H,  $J = 16.0$  Hz, CH=), 4.59-4.61 (d, 2H,  $J = 8.0$  Hz,  $\text{CH}_2$ ), 3.70 (s, 3H,  $\text{OCH}_3$ ), 2.40 (s, 3H,  $\text{CH}_3$ ).

Compound **12f**: Yield 61%, MS (ESI)  $m/z = 448.2$   $[\text{M}+\text{H}]^+$ .  $^1\text{H}$  NMR ( $d_6$ -DMSO, 400 MHz)  $\delta$ : 10.89 (s, 1H, NH), 8.01-8.03 (d, 1H,  $J = 8$  Hz, Ar-H), 7.86-7.89 (m, 2H, Ar-H), 7.56-7.70 (m, 2H, NH, Ar-H), 7.32-7.48 (m, 8H, CH=, Ar-H), 7.09-7.11 (m, 1H, Ar-H), 6.51-6.55 (d, 1H,  $J = 16.0$  Hz, CH=), 4.98 (s, 2H,  $\text{CH}_2$ ), 3.70 (s, 3H,  $\text{OCH}_3$ ), 2.40 (s, 3H,  $\text{CH}_3$ ).

Compound **12g**: Yield 65%, MS (ESI)  $m/z = 464.2$   $[\text{M}+\text{H}]^+$ .  $^1\text{H}$  NMR ( $d_6$ -DMSO, 400 MHz)  $\delta$ : 10.93 (s, 1H, NH), 8.03 (d, 1H,  $J = 8.0$  Hz, Ar-H), 7.61-7.68 (m, 5H, NH, Ar-H), 7.35-7.55 (m,

6H, CH=, Ar-H), 6.99-7.10 (m, 2H, Ar-H), 6.56-6.60 (m, 1H, CH=), 4.97 (s, 2H, CH<sub>2</sub>), 3.70-3.73 (m, 6H, 2 × OCH<sub>3</sub>).

Compound **12h**: Yield 64%. MS (ESI)  $m/z = 464.2$  [M+H]<sup>+</sup>. <sup>1</sup>H NMR (*d*<sub>6</sub>-DMSO, 400 MHz)  $\delta$ : 10.93 (s, 1H, NH), 8.03 (d, 1H,  $J = 8$  Hz, Ar-H), 7.55-8.05 (m, 6H, NH, Ar-H), 7.34-7.50 (m, 5H, CH=, Ar-H), 6.99-7.09 (m, 2H, Ar-H), 6.51-6.55 (d, 1H,  $J = 16.0$  Hz, CH=), 4.97 (s, 2H, CH<sub>2</sub>), 3.70-3.73 (m, 6H, 2 × OCH<sub>3</sub>).

Compound **12i**: Yield 68%. MS (ESI)  $m/z = 464.2$  [M+H]<sup>+</sup>. <sup>1</sup>H NMR (*d*<sub>6</sub>-DMSO, 400 MHz)  $\delta$ : 10.81 (s, 1H, NH), 8.04 (d, 1H,  $J = 8.0$  Hz, Ar-H), 7.61-7.67 (m, 3H, NH, Ar-H), 7.42-7.56 (m, 7H, CH=, Ar-H), 6.99-7.17 (m, 3H, Ar-H), 6.73 (m, 1H, Ar-H), 6.58 (d, 1H,  $J = 16.0$  Hz, CH=), 4.61 (d, 2H,  $J = 4.0$  Hz, CH<sub>2</sub>), 3.71-3.81 (m, 6H, 2 × OCH<sub>3</sub>).

Compound **12j**: Yield 65%. MS (ESI)  $m/z = 464.2$  [M+H]<sup>+</sup>. <sup>1</sup>H NMR (*d*<sub>6</sub>-DMSO, 400 MHz)  $\delta$ : 10.94 (s, 1H, NH), 8.04 (d, 1H,  $J = 8$  Hz, Ar-H), 7.57-7.70 (m, 5H, NH, Ar-H), 7.34-7.51 (m, 6H, CH=, Ar-H), 7.00-7.09 (m, 2H, Ar-H), 6.51-6.55 (m, 1H, CH=), 4.99 (s, 2H, CH<sub>2</sub>), 3.70-3.75 (m, 6H, 2 × OCH<sub>3</sub>).

Compound **12k**: Yield 59%. MS (ESI)  $m/z = 479.2$  [M+H]<sup>+</sup>. <sup>1</sup>H NMR (*d*<sub>6</sub>-DMSO, 400 MHz)  $\delta$ : 11.16 (s, 1H, NH), 8.07-8.39 (m, 5H, Ar-H), 7.61-7.69 (m, 4H, NH, Ar-H), 7.30-7.51 (m, 5H, CH=, Ar-H), 7.11-7.15 (m, 1H, Ar-H), 6.56-6.61 (m, 1H, CH=), 4.99 (s, 2H, CH<sub>2</sub>), 3.70-3.76 (m, 3H, OCH<sub>3</sub>).

Compound **12l**: Yield 65%. MS (ESI)  $m/z = 479.2$  [M+H]<sup>+</sup>. <sup>1</sup>H NMR (*d*<sub>6</sub>-DMSO, 400 MHz)  $\delta$ : 11.16 (s, 1H, NH), 8.08-8.39 (m, 4H, Ar-H), 7.32-7.86 (m, 9H, CH=, NH, Ar-H), 7.11-7.15 (m, 1H, Ar-H), 6.49-6.53 (d, 1H,  $J = 16.0$  Hz, CH=), 5.01 (s, 2H, CH<sub>2</sub>), 3.70-3.72 (s, 3H, OCH<sub>3</sub>).

Compound **12m**: Yield 63%. MS (ESI)  $m/z = 494.2$  [M+H]<sup>+</sup>. <sup>1</sup>H NMR (*d*<sub>6</sub>-DMSO, 400 MHz)  $\delta$ : 10.90 (s, 1H, NH), 8.02 (d, 1H,  $J = 4$  Hz, Ar-H), 7.49-7.73 (m, 5H, NH, Ar-H), 7.38-7.45 (m, 4H, CH=, Ar-H), 7.29 (s, 1H, Ar-H), 7.06-7.10 (m, 2H, Ar-H), 6.56-6.60 (d, 1H,  $J = 16.0$  Hz, CH=), 4.97 (s, 2H, CH<sub>2</sub>), 3.66-3.83 (m, 9H, 3 × OCH<sub>3</sub>).

Compound **12n**: Yield 65%. MS (ESI)  $m/z = 494.2$  [M+H]<sup>+</sup>. <sup>1</sup>H NMR (*d*<sub>6</sub>-DMSO, 400 MHz)  $\delta$ : 10.91 (s, 1H, NH), 8.03 (d, 1H,  $J = 4$  Hz, Ar-H), 7.57-7.70 (m, 4H, NH, Ar-H), 7.31-7.49 (m, 6H, CH=, Ar-H), 7.09-7.12 (m, 2H, Ar-H), 6.51-6.55 (d, 1H,  $J = 16.0$  Hz, CH=), 5.00 (s, 2H, CH<sub>2</sub>), 3.68-3.86 (m, 9H, 3 × OCH<sub>3</sub>).

Compound **12o**: Yield 62%. MS (ESI)  $m/z = 524.2$  [M+H]<sup>+</sup>. <sup>1</sup>H NMR (*d*<sub>6</sub>-DMSO, 400 MHz)  $\delta$ : 10.95 (s, 1H, NH), 8.03-8.05 (d, 1H,  $J = 8$  Hz, Ar-H), 7.58-7.69 (m, 4H, NH, Ar-H), 7.35-7.50 (m, 5H, CH=, Ar-H), 7.07-7.11 (m, 2H, Ar-H), 6.57-6.61 (d, 1H,  $J = 16.0$  Hz, CH=), 4.98 (s, 2H, CH<sub>2</sub>), 3.71-3.76 (m, 12H, OCH<sub>3</sub>).

Compound **12p**: Yield 67%. MS (ESI)  $m/z = 524.2$  [M+H]<sup>+</sup>. <sup>1</sup>H NMR (*d*<sub>6</sub>-DMSO, 400 MHz)  $\delta$ : 10.95 (s, 1H, NH), 8.05-8.07 (d, 1H,  $J = 8$  Hz, Ar-H), 7.57-7.70 (m, 4H, NH, Ar-H), 7.35-7.50 (m,

5H, CH=, Ar-H), 7.08-7.13 (m, 2H, Ar-H), 6.51-6.55 (d, 1H,  $J = 16.0$  Hz, CH=), 5.00 (s, 2H, CH<sub>2</sub>), 3.70-3.83 (m, 12H, OCH<sub>3</sub>).

### 5.3. General preparation of **13a-p**.

A solution of NH<sub>2</sub>OK (0.25 g, 10 mmol) in 6 mL of anhydrous methanol was added to a solution of **12** (1 mmol) in 3 mL of anhydrous methanol. The mixture was stirred for 12 h at room temperature. Upon completion, the mixture was condensed under vacuum, and the residue was neutralized with 2 N HCl to pH = 7, and then concentrated. The residue was purified by column chromatography to afford target compounds **13a-p**.

Compound **13a**: Yield 51%, a pale yellow solid. Purity: 97.9% (by HPLC). MS (ESI)  $m/z = 359.2$  [M+H]<sup>+</sup>; <sup>1</sup>H NMR (*d*<sub>6</sub>-DMSO, 400 MHz)  $\delta$ : 10.90 (s, 1H, NH), 10.33 (s, 1H, NH), 8.86 (s, 1H, Ar-H), 8.59 (s, 1H, Ar-H), 7.94 (d, 1H,  $J = 8.0$  Hz, Ar-H), 7.69-7.73 (m, 4H, NH, Ar-H), 7.45-7.51 (m, 4H, CH=, Ar-H), 7.06 (m, 1H, Ar-H), 6.57 (d, 1H,  $J = 16.0$  Hz, CH=), 4.87 (d, 2H,  $J = 8.0$  Hz, CH<sub>2</sub>). <sup>13</sup>C NMR (*d*<sub>6</sub>-DMSO, 100 MHz)  $\delta$ : 167.2, 151.6, 144.8, 143.2, 139.4, 133.9, 132.9, 131.4, 129.3, 128.9, 128.3, 127.9, 126.7, 122.1, 121.5, 118.5, 117.6, 112.0, 45.5. HRMS (ESI):  $m/z$  calcd for C<sub>21</sub>H<sub>19</sub>N<sub>4</sub>O<sub>2</sub>: 359.1508; found: 359.1522.

Compound **13b**: Yield 47%, a pale yellow solid. Purity: 98.3% (by HPLC). MS (ESI)  $m/z = 359.2$  [M+H]<sup>+</sup>; <sup>1</sup>H NMR (*d*<sub>6</sub>-DMSO, 400 MHz)  $\delta$ : 11.78 (s, 1H, NH), 10.36 (s, 1H, NH), 8.75 (s, 1H, Ar-H), 8.50 (s, 1H, Ar-H), 7.93 (d, 1H,  $J = 8.0$  Hz, Ar-H), 7.63-7.70 (m, 3H, NH, Ar-H), 7.34-7.49 (m, 5H, CH=, Ar-H), 7.05-7.08 (m, 1H, Ar-H), 6.58 (d, 1H,  $J = 16.0$  Hz, CH=), 4.88 (m, 2H, CH<sub>2</sub>). <sup>13</sup>C NMR (*d*<sub>6</sub>-DMSO, 100 MHz)  $\delta$ : 166.7, 151.6, 145.0, 141.2, 139.2, 134.4, 133.2, 131.4, 130.0, 129.3, 129.2, 128.1, 127.8, 127.2, 122.0, 120.7, 118.4, 118.1, 114.4, 112.0, 45.6. HRMS (ESI):  $m/z$  calcd for C<sub>21</sub>H<sub>19</sub>N<sub>4</sub>O<sub>2</sub>: 359.1508; found: 359.1499.

Compound **13c**: Yield 55%, a pale yellow solid. Purity: 98.5% (by HPLC). MS (ESI)  $m/z = 373.2$  [M+H]<sup>+</sup>; <sup>1</sup>H NMR (*d*<sub>6</sub>-DMSO, 400 MHz)  $\delta$ : 10.97 (s, 1H, NH), 7.94 (d, 1H,  $J = 8.0$  Hz, Ar-H), 7.61-7.67 (m, 4H, NH, Ar-H), 7.34-7.43 (m, 3H, CH=, Ar-H), 7.05-7.06 (m, 2H, Ar-H), 6.59 (d, 1H,  $J = 16.0$  Hz, CH=), 4.88 (m, 2H, CH<sub>2</sub>), 3.71 (s, 3H, OCH<sub>3</sub>), 2.63 (s, 3H, CH<sub>3</sub>). <sup>13</sup>C NMR (*d*<sub>6</sub>-DMSO, 100 MHz)  $\delta$ : 167.2, 151.6, 144.8, 143.2, 142.1, 139.3, 133.0, 131.4, 129.3, 128.9, 128.3, 128.1, 125.5, 122.2, 121.6, 118.6, 117.6, 112.1, 45.8, 40.7, 40.5, 40.3, 40.0, 39.8, 39.6, 39.4, 21.0. HRMS (ESI):  $m/z$  calcd for C<sub>22</sub>H<sub>21</sub>N<sub>4</sub>O<sub>2</sub>: 373.1665; found: 373.1673.

Compound **13d**: Yield 50%, a pale yellow solid. Purity: 95.4% (by HPLC). MS (ESI)  $m/z = 373.2$  [M+H]<sup>+</sup>; <sup>1</sup>H NMR (*d*<sub>6</sub>-DMSO, 400 MHz)  $\delta$ : 10.96 (s, 1H, NH), 7.94 (d, 1H,  $J = 8$  Hz, Ar-H), 7.61-7.66 (m, 4H, NH, Ar-H), 7.34-7.42 (m, 4H, NH, CH=, Ar-H), 7.04 (m, 2H, Ar-H), 6.58 (d, 1H,  $J = 16.0$  Hz, CH=), 4.88 (m, 2H, CH<sub>2</sub>), 2.63 (s, 3H, CH<sub>3</sub>). <sup>13</sup>C NMR (*d*<sub>6</sub>-DMSO, 100 MHz)  $\delta$ : 167.0, 151.6, 145.0, 142.2, 141.2, 139.3, 134.4, 131.4, 130.0, 129.4, 129.3, 128.1, 127.8, 127.2, 122.1, 121.6, 118.5, 118.2, 114.4, 112.0, 45.9, 40.7, 40.5, 40.3, 40.0, 39.8, 39.6, 39.4, 21.0. HRMS (ESI):  $m/z$  calcd for C<sub>22</sub>H<sub>21</sub>N<sub>4</sub>O<sub>2</sub>: 373.1665; found: 373.1677.

Compound **13e**: Yield 49%, a pale yellow solid. Purity: 99.1% (by HPLC). MS (ESI)  $m/z = 449.2$  [M+H]<sup>+</sup>; <sup>1</sup>H NMR (*d*<sub>6</sub>-DMSO, 400 MHz)  $\delta$ : 10.81 (s, 1H, NH), 8.04 (d, 1H,  $J = 8.0$  Hz, Ar-H),

7.61-7.68 (m, 4H, NH, Ar-H), 7.35-7.55 (m, 7H, NH, CH=, Ar-H), 7.09-7.17 (m, 2H, Ar-H), 6.72-6.75 (m, 1H, Ar-H), 6.58 (d, 1H,  $J = 16.0$  Hz, CH=), 4.61 (m, 2H, CH<sub>2</sub>), 2.40 (s, 3H, CH<sub>3</sub>). <sup>13</sup>C NMR (*d*<sub>6</sub>-DMSO, 100 MHz)  $\delta$ : 167.2, 151.7, 144.9, 143.3, 143.0, 138.7, 138.0, 136.3, 133.9, 133.0, 129.6, 129.0, 128.7, 128.5, 128.2, 127.7, 122.0, 121.3, 118.9, 117.6, 117.4, 112.5, 45.9, 40.6, 40.4, 40.2, 40.0, 39.8, 39.6, 39.4, 21.4. HRMS (ESI):  $m/z$  calcd for C<sub>28</sub>H<sub>25</sub>N<sub>4</sub>O<sub>2</sub>: 449.1978; found: 449.1991.

Compound **13f**: Yield 53%, a pale yellow solid. Purity: 96.2% (by HPLC). MS (ESI)  $m/z = 449.2$  [M+H]<sup>+</sup>; <sup>1</sup>H NMR (*d*<sub>6</sub>-DMSO, 400 MHz)  $\delta$ : 11.40 (s, 1H, NH), 10.33 (s, 1H, NH), 8.86 (s, 1H, Ar-H), 8.29 (d, 1H,  $J = 8.0$  Hz, Ar-H), 7.57-7.72 (m, 10H, NH, Ar-H), 7.41-7.47 (m, 2H, CH=, Ar-H), 6.52 (d, 1H,  $J = 16.0$  Hz, CH=), 4.98 (m, 2H, CH<sub>2</sub>), 2.39 (s, 3H, CH<sub>3</sub>). <sup>13</sup>C NMR (*d*<sub>6</sub>-DMSO, 100 MHz)  $\delta$ : 167.0, 151.7, 145.1, 143.0, 141.4, 138.7, 138.0, 136.4, 134.5, 133.8, 130.0, 129.6, 129.5, 129.4, 128.5, 127.8, 127.3, 122.0, 121.3, 118.8, 118.1, 112.5, 46.0, 40.6, 40.4, 40.2, 40.0, 39.8, 39.6, 39.4, 21.4. HRMS (ESI):  $m/z$  calcd for C<sub>28</sub>H<sub>25</sub>N<sub>4</sub>O<sub>2</sub>: 449.1978; found: 449.1969.

Compound **13g**: Yield 58%, a pale yellow solid. Purity: 95.3% (by HPLC). MS (ESI)  $m/z = 465.2$  [M+H]<sup>+</sup>; <sup>1</sup>H NMR (*d*<sub>6</sub>-DMSO, 400 MHz)  $\delta$ : 10.94 (s, 1H, NH), 8.03 (d, 1H,  $J = 8.0$  Hz, Ar-H), 7.34-7.68 (m, 11H, NH, CH=, Ar-H), 6.99-7.16 (m, 2H, Ar-H), 6.60 (d, 1H,  $J = 16.0$  Hz, CH=), 4.97 (m, 2H, CH<sub>2</sub>), 3.70-3.73 (m, 3H, OCH<sub>3</sub>). <sup>13</sup>C NMR (*d*<sub>6</sub>-DMSO, 100 MHz)  $\delta$ : 167.2, 159.8, 152.4, 145.3, 143.0, 140.6, 138.3, 133.7, 132.6, 130.0, 128.8, 128.5, 128.2, 128.0, 121.8, 121.1, 120.9, 117.2, 114.6, 113.6, 112.5, 56.0, 45.8, 40.6, 40.4, 40.2, 40.0, 39.8, 39.6, 39.4. HRMS (ESI):  $m/z$  calcd for C<sub>28</sub>H<sub>25</sub>N<sub>4</sub>O<sub>3</sub>: 465.1927; found: 465.1941.

Compound **13h**: Yield 52%, a pale yellow solid. Purity: 96.6% (by HPLC). MS (ESI)  $m/z = 465.2$  [M+H]<sup>+</sup>; <sup>1</sup>H NMR (*d*<sub>6</sub>-DMSO, 400 MHz)  $\delta$ : 10.82 (s, 1H, NH), 8.05 (d, 1H,  $J = 8$  Hz, Ar-H), 7.34-7.70 (m, 9H, NH, CH=, Ar-H), 7.00-7.19 (m, 3H, Ar-H), 6.71 (m, 1H, Ar-H), 6.58-6.62 (d, 1H,  $J = 16.0$  Hz, CH=), 5.00 (s, 2H, CH<sub>2</sub>), 3.71 (s, 3H, OCH<sub>3</sub>). <sup>13</sup>C NMR (*d*<sub>6</sub>-DMSO, 100 MHz)  $\delta$ : 167.1, 159.8, 152.4, 143.0, 141.4, 140.6, 138.3, 134.5, 134.2, 133.7, 130.1, 129.3, 128.5, 128.1, 127.8, 127.6, 127.3, 127.1, 121.1, 120.9, 119.0, 118.4, 114.5, 114.1, 113.8, 112.5, 55.6, 45.9. HRMS (ESI):  $m/z$  calcd for C<sub>28</sub>H<sub>25</sub>N<sub>4</sub>O<sub>3</sub>: 465.1927; found: 465.1938.

Compound **13i**: Yield 55%, a yellow solid. Purity: 99.4% (by HPLC). MS (ESI)  $m/z = 465.2$  [M+H]<sup>+</sup>; <sup>1</sup>H NMR (*d*<sub>6</sub>-DMSO, 400 MHz)  $\delta$ : 10.73 (s, 1H, NH), 9.01 (s, 1H, Ar-H), 8.39-8.41 (d, 1H,  $J = 8.0$  Hz, Ar-H), 8.15-8.17 (m, 2H, NH, Ar-H), 7.40-7.52 (m, 8H, NH, CH=, Ar-H), 7.18-7.20 (m, 3H, Ar-H), 6.67 (m, 1H, Ar-H), 6.40-6.44 (d, 1H,  $J = 16.0$  Hz, CH=), 4.62 (d, 2H,  $J = 4.0$  Hz, CH<sub>2</sub>), 3.89 (s, 3H, OCH<sub>3</sub>). <sup>13</sup>C NMR (*d*<sub>6</sub>-DMSO, 100 MHz)  $\delta$ : 167.2, 152.5, 151.6, 145.2, 143.3, 143.0, 138.6, 133.51, 130.0, 129.7, 128.3, 127.7, 121.2, 114.5, 114.2, 112.5, 55.9, 45.9, 40.6, 40.4, 40.2, 40.0, 39.8, 39.6, 39.4. HRMS (ESI):  $m/z$  calcd for C<sub>28</sub>H<sub>25</sub>N<sub>4</sub>O<sub>3</sub>: 465.1927; found: 465.1919.

Compound **13j**: Yield 50%, a pale yellow solid. Purity: 96.5% (by HPLC). MS (ESI)  $m/z = 465.2$  [M+H]<sup>+</sup>; <sup>1</sup>H NMR (*d*<sub>6</sub>-DMSO, 400 MHz)  $\delta$ : 11.36 (s, 1H, NH), 8.05 (s, 1H, Ar-H), 7.89-7.94 (m, 3H, NH, Ar-H), 7.34-7.67 (m, 7H, NH, CH=, Ar-H), 7.00-7.26 (m, 4H, Ar-H), 6.35-6.39 (d, 1H,  $J$

= 16.0 Hz, CH=), 4.96 (s, 2H, CH<sub>2</sub>), 3.78 (s, 3H, OCH<sub>3</sub>). <sup>13</sup>C NMR (*d*<sub>6</sub>-DMSO, 100 MHz) δ: 167.1, 152.5, 151.7, 145.2, 143.0, 141.4, 138.6, 134.4, 134.2, 133.5, 131.8, 130.2, 130.0, 129.7, 128.4, 127.7, 127.2, 121.8, 121.2, 118.9, 118.3, 114.5, 114.2, 112.5, 55.9, 46.0, 40.6, 40.4, 40.2, 40.0, 39.8, 39.6, 39.4. HRMS (ESI): *m/z* calcd for C<sub>28</sub>H<sub>25</sub>N<sub>4</sub>O<sub>3</sub>: 465.1927; found: 465.1914.

Compound **13k**: Yield 56%, a pale yellow solid. Purity: 95.6% (by HPLC). MS (ESI) *m/z* = 480.2 [M+H]<sup>+</sup>; <sup>1</sup>H NMR (*d*<sub>6</sub>-DMSO, 400 MHz) δ: 11.05 (s, 1H, NH), 8.75 (s, 1H, Ar-H), 8.07-8.39 (m, 5H, NH, Ar-H), 7.61-7.68 (m, 4H, NH, Ar-H), 7.31-7.50 (m, 5H, CH=, Ar-H), 7.13-7.15 (m, 1H, Ar-H), 6.56-6.60 (d, 1H, *J* = 16.0 Hz, CH=), 4.98 (m, 2H, CH<sub>2</sub>). <sup>13</sup>C NMR (*d*<sub>6</sub>-DMSO, 100 MHz) δ: 167.2, 152.7, 147.2, 147.1, 145.0, 144.8, 143.4, 143.1, 134.6, 133.0, 130.3, 129.5, 129.0, 128.8, 128.2, 125.8, 124.1, 122.1, 119.3, 117.7, 112.5, 45.8, 40.7, 40.5, 40.3, 40.1, 39.9, 39.6, 39.4. HRMS (ESI): *m/z* calcd for C<sub>27</sub>H<sub>21</sub>N<sub>5</sub>O<sub>4</sub>: 480.1672; found: 480.1680.

Compound **13l**: Yield 53%, a pale yellow solid. Purity: 96.3% (by HPLC). MS (ESI) *m/z* = 480.2 [M+H]<sup>+</sup>; <sup>1</sup>H NMR (*d*<sub>6</sub>-DMSO, 400 MHz) δ: 11.14 (s, 1H, NH), 8.74 (s, 1H, Ar-H), 8.27-8.40 (m, 4H, NH, Ar-H), 8.09 (d, 1H, *J* = 8.0 Hz, Ar-H), 7.35-7.84 (m, 9H, NH, CH=, Ar-H), 7.13 (m, 1H, Ar-H), 6.51 (d, 1H, *J* = 16.0 Hz, CH=), 5.02 (s, 2H, CH<sub>2</sub>). <sup>13</sup>C NMR (*d*<sub>6</sub>-DMSO, 100 MHz) δ: 167.0, 151.9, 147.2, 145.4, 145.2, 145.0, 143.3, 142.8, 141.2, 135.5, 134.8, 134.5, 130.0, 129.5, 129.0, 128.6, 127.8, 127.4, 125.7, 124.2, 121.2, 119.3, 118.2, 112.5, 45.9, 40.7, 40.5, 40.3, 40.0, 39.9, 39.6, 39.4. HRMS (ESI): *m/z* calcd for C<sub>27</sub>H<sub>21</sub>N<sub>5</sub>O<sub>4</sub>: 480.1672; found: 480.1688.

Compound **13m**: Yield 51%, a yellow solid. Purity: 95.5% (by HPLC). MS (ESI) *m/z* = 495.3 [M+H]<sup>+</sup>; <sup>1</sup>H NMR (*d*<sub>6</sub>-DMSO, 400 MHz) δ: 10.93 (s, 1H, NH), 8.03 (d, 1H, *J* = 8 Hz, Ar-H), 7.56-7.69 (m, 4H, NH, Ar-H), 7.30-7.56 (m, 7H, NH, CH=, Ar-H), 7.09-7.11 (m, 2H, Ar-H), 6.58-6.62 (d, 1H, *J* = 16.0 Hz, CH=), 4.98 (m, 2H, CH<sub>2</sub>), 3.66-3.83 (m, 6H, 2 × OCH<sub>3</sub>). <sup>13</sup>C NMR (*d*<sub>6</sub>-DMSO, 100 MHz) δ: 167.2, 151.6, 149.6, 149.3, 144.8, 143.4, 143.0, 138.7, 133.8, 132.9, 131.9, 130.3, 128.9, 128.4, 128.0, 127.6, 125.8, 121.9, 121.4, 121.0, 118.8, 117.6, 112.6, 112.2, 112.1, 56.2, 55.7, 42.9, 40.7, 40.5, 40.3, 40.0, 39.9, 39.7, 39.4. HRMS (ESI): *m/z* calcd for C<sub>29</sub>H<sub>27</sub>N<sub>4</sub>O<sub>4</sub>: 495.3032; found: 495.3045.

Compound **13n**: Yield 47%, a pale yellow solid. Purity: 99.4% (by HPLC). MS (ESI) *m/z* = 495.3 [M+H]<sup>+</sup>; <sup>1</sup>H NMR (*d*<sub>6</sub>-DMSO, 400 MHz) δ: 10.91 (s, 1H, NH), 8.02 (d, 1H, *J* = 8 Hz, Ar-H), 7.56-7.69 (m, 5H, NH, Ar-H), 7.39-7.54 (m, 5H, NH, CH=, Ar-H), 7.29-7.31 (m, 1H, Ar-H), 7.07-7.11 (m, 2H, Ar-H), 6.57-6.61 (d, 1H, *J* = 16.0 Hz, CH=), 4.98 (s, 2H, CH<sub>2</sub>), 3.66-3.83 (m, 6H, 2 × OCH<sub>3</sub>). <sup>13</sup>C NMR (*d*<sub>6</sub>-DMSO, 100 MHz) δ: 167.0, 151.7, 149.6, 149.3, 145.0, 143.0, 141.5, 138.7, 134.5, 133.8, 131.9, 129.8, 129.4, 128.4, 127.6, 127.2, 125.8, 122.0, 121.4, 121.0, 118.8, 118.2, 112.6, 112.2, 56.2, 55.7, 42.8, 40.7, 40.5, 40.3, 40.0, 39.9, 39.7, 39.4. HRMS (ESI): *m/z* calcd for C<sub>29</sub>H<sub>27</sub>N<sub>4</sub>O<sub>4</sub>: 495.3032; found: 495.3049.

Compound **13o**: Yield 54%, a pale yellow solid. Purity: 98.1% (by HPLC). MS (ESI) *m/z* = 525.2 [M+H]<sup>+</sup>; <sup>1</sup>H NMR (*d*<sub>6</sub>-DMSO, 400 MHz) δ: 10.93 (s, 1H, NH), 8.04 (d, 1H, *J* = 8.0 Hz, Ar-H), 7.61-7.68 (m, 4H, NH, Ar-H), 7.34-7.49 (m, 4H, NH, CH=, Ar-H), 7.09-7.15 (m, 3H, Ar-H), 6.59 (d, 1H, *J* = 16.0 Hz, CH=), 4.98 (s, 2H, CH<sub>2</sub>), 3.71-3.76 (m, 9H, 3 × OCH<sub>3</sub>). <sup>13</sup>C NMR (*d*<sub>6</sub>-DMSO, 100 MHz) δ: 167.2, 159.7, 153.4, 144.9, 143.5, 141.5, 138.8, 134.6, 132.9, 130.8, 129.2, 128.5,

127.8, 127.3, 121.8, 121.2, 118.9, 117.6, 112.5, 106.0, 56.2, 55.7, 45.9, 40.7, 40.5, 40.3, 40.0, 39.9, 39.7, 39.4. HRMS (ESI):  $m/z$  calcd for  $C_{30}H_{29}N_4O_5$ : 525.2183; found: 525.2191.

Compound **13p**: Yield 47%, a pale yellow solid. Purity: 95.9% (by HPLC). MS (ESI)  $m/z$  = 525.2  $[M+H]^+$ ;  $^1H$  NMR ( $d_6$ -DMSO, 400 MHz)  $\delta$ : 10.95 (s, 1H, NH), 8.05 (d, 1H,  $J$  = 8.0 Hz, Ar-H), 7.57-7.69 (m, 4H, NH, Ar-H), 7.36-7.47 (m, 5H, NH, CH=, Ar-H), 7.13 (m, 2H, Ar-H), 6.52 (d, 1H,  $J$  = 16.0 Hz, CH=), 5.00 (s, 2H, CH<sub>2</sub>), 3.70-3.77 (m, 9H, 3  $\times$  OCH<sub>3</sub>).  $^{13}C$  NMR ( $d_6$ -DMSO, 100 MHz)  $\delta$ : 167.1, 159.7, 152.5, 145.2, 143.0, 141.4, 138.6, 134.2, 133.5, 131.8, 130.2, 129.8, 129.5, 129.2, 128.4, 127.8, 127.2, 121.9, 121.2, 118.8, 118.2, 118.0, 114.4, 112.5, 56.2, 55.7, 46.0, 40.6, 40.4, 40.2, 40.0, 39.8, 39.6, 39.4. HRMS (ESI):  $m/z$  calcd for  $C_{30}H_{29}N_4O_5$ : 525.2183; found: 525.2195.

#### 5.4. MTT assay

Human cancer cell lines HepG2, SMMC-7721, HCT116, H1299, Bel7402, and drug-resistant Bel7402/5-FU were purchased from Shanghai Institute of Cell Biology (China). The *in vitro* antiproliferative effects were assessed on related cancer cell lines by the MTT method according to previous reports [46]. The producing MTT-formazan crystals were melt in DMSO (150  $\mu$ L). Then the plates were read through an ELISA plate reader at 570 nm. The inhibitory effect was expressed as percentage. Corresponding IC<sub>50</sub> values were then calculated through GraphPadPrism (4.03).

#### 5.5. HDAC assay.

According to the instructions of the HDAC fluorimetric assay kit (Enzo Life Sciences Inc.), the test compounds at different concentrations were respectively incubated with each HDAC enzyme (HDAC1/3/6/8) in the presence of HDAC substrate (Boc-Lys (Ac)-AMC) at 37 °C for 60 min. The reaction was stopped with the addition of the lysine developer. After 30 min, the fluorimetric emission was recorded in a fluorescence plate reader with excitation (355 nm) and emission (460 nm). The HDAC activity was the percentage of activity relative to the control group. The IC<sub>50</sub> was calculated using GraphPad Prism (4.03).

#### 5.6. Cell apoptosis analysis by flow cytometry assay

After overnight culture of Bel7402/5-FU cells, **13p** (2.0 and 5.0  $\mu$ M), SAHA (5.0  $\mu$ M), harmine (20  $\mu$ M), or vehicle were incubated with the cells for 72h. The cells were harvested and then stained with APC-Annexin V and 7-AAD at 37 °C for 15 min. Flow cytometry analysis (Calibur, BD, USA) was used to determine the percentage of apoptotic cells, using APC signal (FL4) (excitation = 633 nm; emission = 660 nm) and 7-AAD staining signal (FL3) (excitation = 488 nm; emission = 647 nm). The data were analyzed using WinList 3D (7.1) and the histogram was plotted using Excel 2016.

#### 5.7. Acridine orange staining

AO was always used to detect them acidic cellular compartment, which emits bright red fluorescence in acidic autophagic vacuole vesicles, but green fluoresces in the cytoplasm and nucleus. After overnight culture of Bel7402/5-FU cells, different concentrations of **13p** (2.0 and 5.0  $\mu$ M), SAHA (5.0  $\mu$ M), harmine (20  $\mu$ M), or vehicle were treated with Bel7402/5-FU cells for

72h. After treatment, cells were incubated with 1 mg/mL AO for 15 min. Then, the AO was removed and observed using a fluorescence microscopy.

#### 5.8. Western blotting assay

Western blotting assay was employed to determine the activity of HDAC, apoptosis-related proteins, and autophagy proteins. Briefly, Bel7402/5-FU cells at  $1.5 \times 10^5$ /mL were plated in 6 cm dishes to incubate for one day. Then the cells were treated with or without SAHA, harmine, or **13p** at different concentrations for 72h. After harvested and lyzed, the cell lysates (50  $\mu$ g/lane) were separated by SDS-PAGE (12% gel) and transferred onto nitrocellulose membranes. When 5% fat-free milk was used to block reaction, the target proteins were probed with anti-Ac-histone H3, anti-Ac-histone H4, anti-Ac- $\alpha$ -tubulin, anti-Bax, anti-Bcl2, anti-H2AX (S139ph), anti-LC3, anti-p62, and anti- $\beta$ -actin antibodies (Cell Signaling Technology, MA, USA), respectively. The bound antibodies were investigated using peroxidase-conjugated secondary antibodies for 1 h, and then conceived by improved chemiluminescent reagent.

#### CONFLICT OF INTEREST

The authors declare no conflict of interest, financial or otherwise.

#### ACKNOWLEDGEMENTS

This work was financially supported by the Natural Science Foundation of China (Nos. 81302628 and 81473089), the Project of “Jiangsu Six Peaks of Talent” (2014-SWYY-044 and 2016-SWYY-CXTD-008), China and Jiangsu Province Postdoctoral Science Foundation (2018T110533, 2016M590488, and 1601136B), the Project of “Jiangsu 333 high-level talents”, and also thank Applied Research Projects of Nantong City.

#### References

- [1] World Health Organization Report, 2016. <http://www.who.int/cancer/en/>.
- [2] J.G. Chen, T.W. Kensler, Changing rates for liver and lung cancers in Qidong, China, *Chem. Res. Toxicol.* 27 (2014) 3-6.
- [3] X. Ma, M. Hu, H. Wang, J. Li, Discovery of traditional Chinese medicine monomers and their synthetic intermediates, analogs or derivatives for battling P-gp-mediated multi-drug resistance. *Eur. J. Med. Chem.* 159 (2018) 381-392.
- [4] S. Vijayaraghavalu, C. Peetla, S. Lu, V. Labhasetwar, Epigenetic modulation of the biophysical properties of drug-resistant cell lipids to restore drug transport and endocytic functions, *Mol. Pharm.* 9 (2012) 2730.
- [5] M.L. Han, Y.F. Zhao, C.H. Tan, Y.J. Xiong, W.J. Wang, F. Wu, Y. Fei, L. Wang, Z.Q. Liang, Cathepsin L upregulation-induced EMT phenotype is associated with the acquisition of cisplatin or paclitaxel resistance in A549 cells, *Acta Pharmacol. Sin.* 37 (2016) 1606-1622.
- [6] J. Huang, H. Mei, Z. Tang, J. Li, X. Zhang, Y. Lu, F. Huang, Q. Jin, Z. Wang, Triple-amiRNA VEGFRs inhibition in pancreatic cancer improves the efficacy of chemotherapy through EMT regulation, *J. Control Release.* 245 (2017) 1-14.

- [7] (a) H. Kakeya, Natural products-prompted chemical biology: phenotypic screening and a new platform for target identification, *Nat. Prod. Rep.* 33 (2016) 648. (b) D.J. Newman, G.M. Cragg, Natural Products as Sources of New Drugs from 1981 to 2014, *J. Nat. Prod.* 79 (2016) 629–661.
- [8] G.M. Gragg, P.G. Grothaus, D.J. Newman, Impact of natural products on developing new anti-cancer agents, *Chem. Rev.* 109 (2009) 3012–3043.
- [9] H. Huang, Y. Yao, Z. He, T. Yang, J. Ma, X. Tian, Y. Li, C. Huang, X. Chen, W. Li, S. Zhang, C. Zhang, J. Ju, Antimalarial  $\beta$ -carboline and indolactam alkaloids from *Marinactinospora* thermotolerans, a deep sea isolate, *J. Nat. Prod.* 74 (2011) 2122.
- [10] A. Laine, C. Lood, A. Koskinen, Pharmacological importance of optically active tetrahydro- $\beta$ -carbolines and synthetic approaches to create the C1 stereocenter, *Molecules.* 19 (2014) 1544-67.
- [11] R. Cao, W. Peng, Z. Wang, A. Xu, Beta-Carboline alkaloids: biochemical and pharmacological functions, *Curr. Med. Chem.* 14 (2007) 479-500.
- [12] V. Vishwakarma, J. New, D. Kumar, V. Snyder, L. Arnold, E. Nissen, Q. Hu, N. Cheng, D. Miller, A.R. Thomas, Y. Shnayder, K. Kakarala, T.T. Tsue, D.A. Girod, S.M. Thomas, Potent Antitumor Effects of a Combination of Three Nutraceutical Compounds, *Sci. Rep.* 8 (2018) 12163.
- [13] S. Kumar, A. Singh, K. Kumar, V. Kumar, Recent insights into synthetic  $\beta$ -carbolines with anti-cancer activities, *Eur. J. Med. Chem.* 142 (2017) 48-73.
- [14] Y. Ling, C.J. Xu, L. Luo, J. Cao, J. Feng, Y. Xue, Q. Zhu, C. Ju, F. Li, Y.A. Zhang, X. Ling, Novel  $\beta$ -Carboline/Hydroxamic Acid Hybrids Targeting Both Histone Deacetylase and DNA Display High Anticancer Activity via Regulation of the p53 Signaling Pathway, *J. Med. Chem.* 58 (2015) 9214-9227.
- [15] Y. Ling, J. Feng, L. Luo, J. Guo, Y.F. Peng, T.T. Wang, X. Ge, Q. Xu, X. Wang, H. Dai, Y.A. Zhang, Design and synthesis of novel C3-sustituted  $\beta$ -carboline-based HDAC inhibitors with potent antitumor activities, *Chem. Med. Chem.* 12 (2017) 646-651.
- [16] Y. Ma, M. Wink, The beta-carboline alkaloid harmine inhibits BCRP and can reverse resistance to the anticancer drugs mitoxantrone and camptothecin in breast cancer cells, *Phytother Res.* 24 (2010) 146-9.
- [17] R.G. Fu, Y. Sun, W.B. Sheng, D.F. Liao, Designing multi-targeted agents: An emerging anticancer drug discovery paradigm, *Eur. J. Med. Chem.* 136 (2017) 195-211.
- [18] P.G. Richardson, P. Moreau, J.P. Laubach, M.E. Maglio, S. Lonial, J. San-Miguel, Deacetylase inhibitors as a novel modality in the treatment of multiple myeloma, *Pharmacol Res.* 117 (2017) 185-191.
- [19] H.T. Qin, H.Q. Li, F.Liu, Selective histone deacetylase small molecule inhibitors: recent progress and perspectives, *Expert Opin. Ther. Pat.* 27 (2017) 621-636.
- [20] K.K. To, W.S. Tong, L.W. Fu, Reversal of platinum drug resistance by the histone deacetylase inhibitor belinostat, *Lung Cancer.* 103 (2017) 58-65.
- [21] A. Suraweera, K.J. O'Byrne, D.J. Richard, Combination therapy with histone deacetylase inhibitors (HDACi) for the treatment of cancer: achieving the full therapeutic potential of HDACi, *Front Oncol.* 8 (2018) 92.
- [22] N. Garpmpis, C. Damaskos, A. Garpmpis, D. Dimitroulis, E. Spartalis, G.A. Margonis, D. Schizas, I. Deskou, C. Doula, E. Magkouti, N. Andreatos, E.A. Antoniou, A. Nonni, K.

- Kontzoglou, D. Mantas, Targeting histone deacetylases in malignant melanoma: A future therapeutic agent or just great expectations? *Anticancer Res.* 37 (2017) 5355-5362.
- [23] G. Mariño, M. Niso-Santano, E.H. Baehrecke, G. Kroemer. Self-consumption: the interplay of autophagy and apoptosis, *Nat. Rev. Mol. Cell Biol.* 15 (2014) 81–94.
- [24] M.S. Gilardini Montani, M. Granato, C. Santoni, P. Del Porto, N. Merendino, G. D'Orazi, A. Faggioni, M. Cirone, Histone deacetylase inhibitors VPA and TSA induce apoptosis and autophagy in pancreatic cancer cells, *Cell Oncol. (Dordr).* 40 (2017) 167-180.
- [25] H. Rikiishi, Autophagic and apoptotic effects of HDAC inhibitors on cancer cells. *J. Biomed. Biotechnol.* 2011 (2011) 830260.
- [26] N. Gammoh, D. Lam, C. Puente, I. Ganley, P.A. Marks, X. Jiang, Role of autophagy in histone deacetylase inhibitor-induced apoptotic and nonapoptotic cell death, *Proc. Natl. Acad. Sci. USA* 109 (2012) 6561–6565.
- [27] X.Y. Sun, Y. Qu, A.R. Ni, G.X. Wang, W.B. Huang, Z.P. Chen, Z.F. Lv, S. Zhang, H. Lindsay, S. Zhao, X.N. Li, B.H. Feng, Novel histone deacetylase inhibitor N25 exerts anti-tumor effects and induces autophagy in human glioma cells by inhibiting HDAC3. *Oncotarget* 8 (2017) 75232-75242.
- [28] N. Zou, Y. Wei, F. Li, Y. Yang, X. Cheng, C. Wang, The inhibitory effects of compound Muniziqi granule against B16 cells and harmine induced autophagy and apoptosis by inhibiting Akt/mTOR pathway. *BMC Complement Altern. Med.*, 17 (2017) 517.
- [29] C. Li, Y. Wang, C. Wang, X. Yi, M. Li, X. He, Anticancer activities of harmine by inducing a pro-death autophagy and apoptosis in human gastric cancer cells. *Phytomedicine* 28 (2017) 10-18.
- [30] T.R. Wilson, P.G. Johnston, D.B. Longley, Anti-apoptotic mechanisms of drug resistance in cancer, *Curr. Cancer Drug Targets.* 9 (2009) 307–319.
- [31] Y. Gou, Z. Zhang, D. Li, L. Zhao, M. Cai, Z. Sun, Y. Li, Y. Zhang, H. Khan, H. Sun, T. Wang, H. Liang, F. Yang, HSA-based multi-target combination therapy: regulating drugs' release from HSA and overcoming single drug resistance in a breast cancer model, *Drug Deliv.* 25 (2018) 321-329.
- [32] H.Y. Yang, L. Zhao, Z. Yang, Q. Zhao, L. Qiang, J. Ha, Z.Y. Li, Q.D. You, Q.L. Guo, Oroxylin A reverses multi-drug resistance of human hepatoma BEL7402/5-FU cells via downregulation of P-glycoprotein expression by inhibiting NF- $\kappa$ B signaling pathway, *Mol. Carcinog.* 51 (2012):185-95.
- [33] J.H. Lee, J.H. Park, Y. Jung, J.H. Kim, H.S. Jong, T.Y. Kim, Y.J. Bang, Histone deacetylase inhibitor enhances 5-fluorouracil cytotoxicity by down-regulating thymidylate synthase in human cancer cells, *Mol. Cancer Ther.* 5 (2006) 3085-3095.
- [34] K. Okada, S. Hakata, J. Terashima, T. Gamou, W. Habano, S. Ozawa, Combination of the histone deacetylase inhibitor depsipeptide and 5-fluorouracil upregulates major histocompatibility complex class II and p21 genes and activates caspase-3/7 in human colon cancer HCT-116 cells, *Oncol. Rep.* 36 (2016) 1875–1885.
- [35] T. Minegaki, A. Suzuki, M. Mori, S. Tsuji, S. Yamamoto, A. Watanabe, T. Tsuzuki, T. Tsunoda, A. Yamamoto, M. Tsujimoto, K. Nishiguchi, Histone deacetylase inhibitors sensitize 5-fluorouracil-resistant MDA-MB-468 breast cancer cells to 5-fluorouracil, *Oncol. Lett.* 16 (2018) 6202–6208.
- [36] R. Hamam, D. Ali, R. Vishnubalaji, Z.F. Alsaaran, E.P. Chalisserry, M. Alfayez, A.

- Aldahmash, N.M. Alajez, Enhanced efficacy of 5-fluorouracil in combination with a dual histone deacetylase and phosphatidylinositide 3-kinase inhibitor (CUDC-907) in colorectal cancer cells, *Saudi. J. Gastroenterol.* 23 (2017) 34–38.
- [37] O. Witt, H.E. Deubzer, T. Milde, I. Oehme, HDAC family: What are the cancer relevant targets? *Cancer Lett.* 277 (2009) 8-21.
- [38] M. Paris, M. Porcelloni, M. Binaschi, et al., Histone deacetylase inhibitors: From bench to clinic, *J. Med. Chem.* 51 (2008) 1505–1529.
- [39] J. Chen, Z. Sang, Y. Jiang, C. Yang, L. He, Design, synthesis, and biological evaluation of quinazoline derivatives as dual HDAC1 and HDAC6 inhibitors for the treatment of cancer. *Chem Biol Drug Des.* 2018, 10.1111/cbdd.13405.
- [40] S.S. Chauhan, A.K. Singh, S. Meena, M. Lohani, A. Singh, R.K. Arya, S.H. Cheruvu, J. Sarkar, J.R. Gayen, D. Datta, P.M. Chauhan, Synthesis of novel  $\beta$ -carboline based chalcones with high cytotoxic activity against breast cancer cells, *Bioorg. Med. Chem. Lett.* 24 (2014) 2820-2824.
- [41] E. White, The role for autophagy in cancer, *J. Clin. Invest.* 125 (2015) 42-46.
- [42] E. White, Deconvoluting the context-dependent role for autophagy in cancer, *Nat. Rev. Cancer.* 12 (2012) 401–410.
- [43] Y. Lu, R. Zhang, S. Liu, Y. Zhao, J. Gao, L. Zhu, ZT-25, a new vacuolar H(+)-ATPase inhibitor, induces apoptosis and protective autophagy through ROS generation in HepG2 cells, *Eur. J. Pharmacol.* 771 (2016) 130-8.
- [44] F. Wang, H. Ma, Z. Liu, W. Huang, X. Xu, X. Zhang,  $\alpha$ -Mangostin inhibits DMBA/TPA-induced skin cancer through inhibiting inflammation and promoting autophagy and apoptosis by regulating PI3K/Akt/mTOR signaling pathway in mice, *Biomed. Pharmacother.* 92 (2017) 672-680.
- [45] W.S. Laitonjam, B. Thingom, S.D. Moirangthem, Indium-mediated michael addition of methyl (Z)-2-(Bromomethyl)-3-phenylacrylate to arylidenemalononitriles in aqueous medium, *Org. Prep. Proced. Int.* 45 (2013) 246-251.
- [46] Y. Ling, J. Guo, Q. Yang, P. Zhu, J. Miao, W. Gao, Y. Peng, J. Yang, K. Xu, B. Xiong, G. Liu, J. Tao, L. Luo, Q. Zhu, Y. Zhang, Development of novel  $\beta$ -carboline-based hydroxamate derivatives as HDAC inhibitors with antiproliferative and antimetastatic activities in human cancer cells, *Eur. J. Med. Chem.* 144 (2018) 398-409.

## **$\beta$ -Carboline and *N*-hydroxycinnamamide hybrids as anticancer agents for drug-resistant hepatocellular carcinoma**

Yong Ling <sup>a,b</sup>, Wei-Jie Gao <sup>a</sup>, Changchun Ling <sup>a,b</sup>, Ji Liu <sup>a</sup>, Chi Meng <sup>a</sup>, Jianqiang Qian <sup>a</sup>, Siqun Liu <sup>a</sup>, Huiling Gan <sup>a</sup>, Hongmei Wu <sup>a</sup>, Jinhua Tao <sup>a</sup>, Hong Dai <sup>a,c,\*</sup>, Yanan Zhang <sup>a,\*</sup>

<sup>a</sup>School of Pharmacy and Jiangsu Province Key Laboratory for Inflammation and Molecular Drug Target, Nantong University, Nantong 226001, PR China.

<sup>b</sup>The Affiliated Hospital of Nantong University, Nantong University, Nantong 226001, PR China.

<sup>c</sup>College of Chemistry and Chemical Engineering, Nantong University, Nantong 226019, PR China

### **Highlights**

1. Novel  $\beta$ -carboline/*N*-hydroxycinnamamide hybrids **13a-p** were designed and synthesized.
2. **13p** demonstrated the highest anticancer potency against drug-sensitive and drug-resistant cells.
3. **13p** displayed HDAC1/6 selective inhibition and increased the Ac-H3, Ac-H4 and Ac- $\alpha$ -tubulin.
4. **13p** triggered more potent apoptosis than SAHA by regulating apoptotic proteins expression.
5. **13p** induced significant autophagy by up-regulation of LC3-II and down-regulation of LC3-I and p62.